Supplemental Table S1.

***P. falciparum* gene identifier**	***P. berghei* gene identifier**	**Protein superfamily**	**PlasmoDB name (if given)**	**Conserved domain (s)**	**Reference (s)**
PF3D7_0629700	PBANKA_1128500	SET	SET domain protein, putative (SET1)	i) SET-domain ii) PHD-domain iii) Bromodomain iv) HDAC interaction domain	(Cui *et al.*, 2008; Volz *et al.*, 2010; Duffy *et al.*, 2013)
PF3D7_1322100	----	SET	Histone-lysine N-methyltransferase SET2 (SET2/*Pf*SETvs) **$**	i) SET-domain ii) PHD-domain	(Cui *et al.*, 2008; Jiang *et al.*, 2013)
PF3D7_0827800	PBANKA_0702900	SET	SET domain protein, putative (SET3)	i) SET-domain ii) Pre-SET domain	(Cui *et al.*, 2008; Jiang *et al.*, 2013)
PF3D7_0910000	PBANKA_0811200	SET	SET domain protein, putative (SET4)	i) SET-domain	(Cui *et al.*, 2008; Volz *et al.*, 2010; Jiang *et al.*, 2013)
PF3D7_1214200	PBANKA_1430000	SET	Histone-lysine N-methyltransferase (SET5)	i) SET-domain	(Cui *et al.*, 2008; Volz *et al.*, 2010; Jiang *et al.*, 2013)
PF3D7_1355300	PBANKA_1131800	SET	Histone-lysine N-methyltransferase (SET6)	i) SET-domain	(Cui *et al.*, 2008; Volz *et al.*, 2010; Jiang *et al.*, 2013)

PF3D7_1115200	PBANKA_0932500	SET	Histone-lysine N-methyltransferase SET7 (SET7) **$**	i)	SET-domain	(Cui *et al.*, 2008; Jiang *et al.*, 2013; Chen *et al.*, 2016)
PF3D7_0403900	PBANKA_1001600	SET	SET domain protein, putative (SET8)	i) ii)	SET-domain PHD-domain	(Cui *et al.*, 2008; Volz *et al.*, 2010; Jiang *et al.*, 2013)
PF3D7_0508100	PBANKA_1107700	SET	SET domain protein, putative (SET9)	i) ii) iii)	Ankyrin repeats Fis1 C-terminal tetratricopeptide repeat DUF2198	(Jiang *et al.*, 2013)
PF3D7_1221000	PBANKA_1436200	SET	Histone-lysine N-methyltransferase, H3 lysine-4 specific (SET10) **$**	i) ii)	SET-domain PHD-domain	(Volz *et al.*, 2012)
PF3D7_1211600	PBANKA_0610100	HKDM	Lysine-specific histone demethylase 1, putative (LSD1)	i) ii) iii) iv)	PHD-domain PHD-like zinc-binding domain FAD-binding domain (x2) NAD(P)-binding Rossmann-like domain	(Cui *et al.*, 2008; Volz *et al.*, 2010; Jiang *et al.*, 2013)
PF3D7_0801900	PBANKA_1228300	HKDM	Lysine-specific histone demethylase, putative (LSD2)	i) ii) iii)	FAD-NAD(P)-binding domain NAD(P)-binding Rossmann-like domain FAD-binding domain (x2)	(Poran *et al.*, 2017)

				iv)	Alanine dehydrogenase/PNT, C-terminal domain	
PF3D7_0809900	----	HKDM	JmjC domain-containing protein, putative (JmjC1)	i) ii) iii)	JmjC domain (x2) JmjN domain C5HC2 -like zinc finger domain	(Cui *et al.*, 2008; Volz *et al.*, 2010; Jiang *et al.*, 2013; Rono *et al.*, 2017)
PF3D7_0602800	PBANKA_0101600	HKDM	JmjC domain-containing protein, putative (JmjC2)	i)	Cupin-like domain	(Cui *et al.*, 2008; Jiang *et al.*, 2013; Rono *et al.*, 2017)
PF3D7_1426200	PBANKA_1018400	Class I PRMT	Protein arginine N-methyltransferase 1 (PRMT1)	i)	Arginine methyltransferase domain	(Horrocks *et al.*, 2009)
PF3D7_0811500	PBANKA_1426000	Class I PRMT	Histone-arginine methyltransferase CARM1, putative	i)	Arginine methyltransferase domain	(Horrocks *et al.*, 2009)
PF3D7_1361000	PBANKA_1137100	Class II PRMT	protein arginine N-methyltransferase 5, putative (PRMT5)	i) ii) iii)	PRMT5 arginine-N-methyltransferase domain PRMT5 TIM barrel domain PRMT5 oligomerisation domain	(Horrocks *et al.*, 2009)

PF3D7_1003300	PBANKA_1201700	GNAT	N-terminal acetyltransferase A complex catalytic subunit ARD1, putative (ARD1)	i)	Acetyltransferase domain	(Kanyal *et al.*, 2018)
PF3D7_0109500	PBANKA_0204100	GNAT	N-acetyltransferase, putative	i) ii)	Acetyltransferase domain FR-47-like domain	(Kanyal *et al.*, 2018)
PF3D7_0805400	PBANKA_1225200	GNAT	Acetyltransferase, putative	i) ii)	Acetyltransferase domain RimL domain	(Kanyal *et al.*, 2018)
PF3D7_0629000	PBANKA_1127600	GNAT	N-acetyltransferase, putative	i)	Acetyltransferase domain	(Kanyal *et al.*, 2018)
PF3D7_1437000	PBANKA_0611800	GNAT	N-acetyltransferase, putative	i) ii)	Acetyltransferase domain NAT domain	(Kanyal *et al.*, 2018)
PF3D7_0823300	PBANKA_0707300	GNAT	Histone acetyltransferase GCN5 (GCN5)	i) ii)	Acetyltransferase domain Bromodomain	(Fan, An and Cui, 2004b, 2004a; Kumar *et al.*, 2017; Kanyal *et al.*, 2018)
PF3D7_1323300	PBANKA_1338500	GNAT	Acetyltransferase, GNAT family, putative	i)	Acetyltransferase domain	(Kanyal *et al.*, 2018)
PF3D7_1227800	PBANKA_1442500	GNAT	Elongator complex protein 3, putative (ELP3)	i)	Radical SAM/HAT domain	(Stilger and Sullivan, 2013; Kanyal *et al.*, 2018)

PF3D7_1020700	PBANKA_0504900	GNAT	Histone acetyltransferase, putative	i) ii) iii) iv)	Acetyltransferase domain Helicase domain tRNA-binding domain tRNA(Met) cytidine acetyltransferase TmcA domain	(Kanyal *et al.*, 2018)
PF3D7_1118600	PBANKA_0929500	MYST	Histone acetyltransferase (MYST) **$**	i) ii) iii)	Acetyltransferase domain Chromodomain-like domain C2HC-type zinc finger domain	(Miao *et al.*, 2010; Kanyal *et al.*, 2018)
PF3D7_0416400	PBANKA_0718400	GNAT	Histone acetyltransferase, putative (HAT1)	i)	HAT1 domain (x2)	(Horrocks *et al.*, 2009)
PF3D7_1472200	PBANKA_1335400	HDAC Class II	Histone deacetylase, putative (HDA1)	i) ii)	Histone deacetylase domain (x3) Ankyrin repeats	(Kanyal *et al.*, 2018)
PF3D7_0506600	PBANKA_1106200	HDAC Class II	Histone deacetylase, putative, pseudogene	i)	Histone deacetylase domain	(Kanyal *et al.*, 2018)
PF3D7_1008000	PBANKA_1206200	HDAC Class II	Histone deacetylase 2 (HDA2/HDAC2) **$**	i) ii) iii)	Histone deacetylase domain (x3) DUF2981 domain Inositol polyphosphate kinase domain	(Coleman *et al.*, 2014; Kanyal *et al.*, 2018)

PF3D7_1023900	PBANKA_0508100	Unclassified	Chromodomain-helicase-DNA-binding protein 1 homolog, putative (CHD1)	i) ii) iii) iv)	Chromo/chromo-shadow domain-like Helicase family ATP-binding domain SNF2-related, N-terminal domain Helicase domain	(Kanyal *et al.*, 2018)
PF3D7_0925700	PBANKA_0826500	HDAC Class I	Histone deacetylase 1 (HDAC1)	i)	Histone deacetylase domain	(Joshi *et al.*, 1999; Chaal *et al.*, 2010; Kanyal *et al.*, 2018)
PF3D7_1328800	PBANKA_1343800	HDAC Class III	Transcriptional regulatory protein SIR2A (SIR2A) **$**	i)	DHS-like NAD/FAD binding/sirtuin domain	(Merrick *et al.*, 2010; Zhu *et al.*, 2012; Mancio-Silva *et al.*, 2013; Kanyal *et al.*, 2018)
PF3D7_1451400	PBANKA_1315100	HDAC Class III	Transcriptional regulatory protein SIR2B (SIR2B) **$**	i)	Histone deacetylase domain (x2)	(Tonkin *et al.*, 2009; Petter *et al.*, 2011; Merrick *et al.*, 2012; Kanyal *et al.*, 2018)
PF3D7_1117100	PBANKA_0930900	UCH	Deubiquinating/deneddylating enzyme (UCH54) **$**	i) ii)	UCH family 1 domain (x2) Menin-binding domain	(Artavanis-Tsakonas *et al.*, 2006; Cui and Miao, 2010)
PF3D7_1460400	PBANKA_1324100	UCH	Ubiquitin carboxyl-terminal hydrolase isozyme L3 (UCHL3) **$**	i)	UCH family 1 domain	(Artavanis-Tsakonas *et al.*, 2010; Cui and Miao, 2010)

PF3D7_1414400	PBANKA_1028300	PP1	Serine/threonine protein phosphatase PP1	i) ii)	Calcineurin-like phosphoesterase domain Serine-threonine protein phosphatase N-terminal domain	(Shimada *et al.*, 2010; Fréville *et al.*, 2012)
PF3D7_1220900	PBANKA_1436100	HP1	Heterochromatin protein 1 (HP1) **$**	i)	Chromo domain	(Brancucci *et al.*, 2014)
PF3D7_1033700	PBANKA_0517500	BDP	Bromodomain protein 1 (BDP1) **$**	i) ii)	Ankyrin repeat region Bromodomain	(Josling *et al.*, 2015)
PF3D7_1212900	PBANKA_1428900	BDP	Bromodomain protein 2, putative (BDP2)	i)	Bromodomain	(Josling *et al.*, 2015)

Supplemental Table S1: Proven and putative epigenetic modifiers in *Plasmodium spp*. This table provides a list of all of the epigenetic modifiers so far identified in *P. falciparum* and *P. berghei* ANKA (where present). The *P. berghei ANKA* genome does not encode for a SET2 histone lysine demethylase or a JmjC1 histone lysine demethylase, though both are present in *P. falciparum*. Gene identifiers (from PlasmoDB) are provided in the first and second columns; the protein superfamily into which the modifying enzymes are classified are provided in the third column; the fourth column contains the PlasmoDB name provided for epigenetic modifier; and the fifth and sixth columns provide a list of protein domains for a given epigenetic modifier with references to studies in which the protein was identified or characterized (characterised in *Plasmodium* or other organism). A "**$**" symbol next to the name of the protein in the fourth column indicates that the protein has been characterised in a *Plasmodium spp*. parasite previously. Only one putative serine/threonine phosphatase (PP1) has been listed as this is the only *Plasmodium* phosphatase with a homologous protein that has been demonstrated as having an effect on histone phosphorylation (Shimada *et al.*, 2010). Table generated using PlasmoDB [up-to-date as of the 4th of March, 2018] (The EuPathDB Project Team, 2018). HKMT: histone lysine methyltransferase; SET: Su(var)3-9, Enhancer of zeste, and Trithorax; HKDM: histone lysine demethylase; PRMT: Protein arginine methyltransferase; PP1: Protein phosphatase 1; GNAT: Gcn5-related *N*-acetyltransferase; HAT: histone acetyltransferase; MYST: MOZ, Ybf1/Sas3, Sas2, and Tip60; HDAC/HDA: Histone deacetylase; ELP: Elongator complex protein; SIR2: Silencing information regulator 2; CHD: Chromodomain helicase DNA-

binding; SNF2: Sucrose non-fermentation 2; DUF: Domain of Unknown Function; TmcA: tRNA(met) cytidine Acetyltransferase; NAT: *N*-acetyltransferase; NAD: nicotinamide adenine dinucleotide; FAD: flavin adenine dinucleotide; DHS: deoxyhypusine synthase; UCH: ubiquitin C-terminal hydrolase.; Chromo: Chromatin Organisation Modifier; SAM: S-adenosylmethionine; JmjC: Jumonji C-terminal; JmjN: Jumonji N-terminal; CARM1: Coactivator-Associated Arginine Methyltransferase 1; Fis1: Mitochondrial Fission protein 1; BDP: Bromodomain protein.

Supplemental Images S1A-S1M: Chapter 3 linear plasmid maps.

i) Linear plasmid pL1186

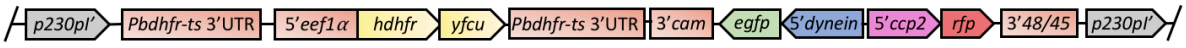

ii) *P. berghei* ANKA high-producer (HP) *p230pl* locus

iii) Integration of linear plasmid after positive selection with Pyrimethamine (820cl1 line)

iv) Integration of linear plasmid after negative selection with 5-fluorocytosine (820cl1m1cl1 line a.k.a "820")

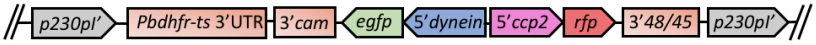

Supplemental Image 1A: The "820" background line. To create a *P. berghei* ANKA line in which male and female gametocytes could be identified by fluorescence, a drug-selectable cassette was inserted at the *p230p* locus (site *p230pl*) (an upstream paralogue of the P230 6-cysteine male gametocyte surface protein; PBANKA_0306000) of the high-producer (HP) *P. berghei* ANKA line, clone15cy1 (Janse et al., 1989; Ponzi et al., 2009). **i)** shows linearised plasmid pL1186. Complementary *p230pl* sequences flanked the drug selection and fluorescent marker cassette (*p230p'* sequences). A fused human dihydrofolate reductase gene (*hdhfr*) with a Pyrimethamine resistance-conferring single nucleotide polymorphism (SNP), and bifunctional yeast cytosine deaminase-uridyl-phosphoribosyltransferase (*ycfu*) acted as the positive/negative drug selection gene. This fused *hdhfr::yfcu* was driven by the 5' promoter of the constitutively-expressed *P. berghei* elongation factor 1 alpha (*5'eef1α*) (bidirectional promoter of genes PBANKA_1133300 and PBANKA_1133400), and flanked by identical 3'UTRs of the mutated *P. berghei* DHFR-TS gene (*pbdhfr-ts 3'UTR*). To produce RFP-fluorescent female gametocytes and GFP-fluorescent male gametocytes, an enhanced green fluorescent protein (*egfp*) sequence was driven by the promoter of the highly male gametocyte-specific heavy dynein chain protein (PBANKA_0416100). A red fluorescent protein sequence (*rfp*) was similarly driven by the promoter of the female gametocyte-specific LCCL-domain containing gene, Ccp2 (*ccp2*) (PBANKA_1319500). This fused fluorescence cassette was then flanked by the 3' UTRs of the *P. berghei* calmodulin gene (*3'cam;* PBANKA_0514800*)* and p48/45 gene (*3' 48/45*). **ii)** and **iii)** illustrate the *p230p* locus (site *p230pl*) of *P. berghei* parasites before and after integration of the plasmid construct. Under Pyrimethamine drug selection, wild-type (WT) parasites such as **ii)** will be killed by the drug, leaving only parasites with integrated selection cassettes such as **iii).** The final *p230p* locus in **iv)** depicts the "820" background clonal line after negative selective with 5-fluorocytosine (5-FC), which has led to a recombination event in which the drug selectable cassette has been lost, but the fluorescent GFP/RFP cassette remains.

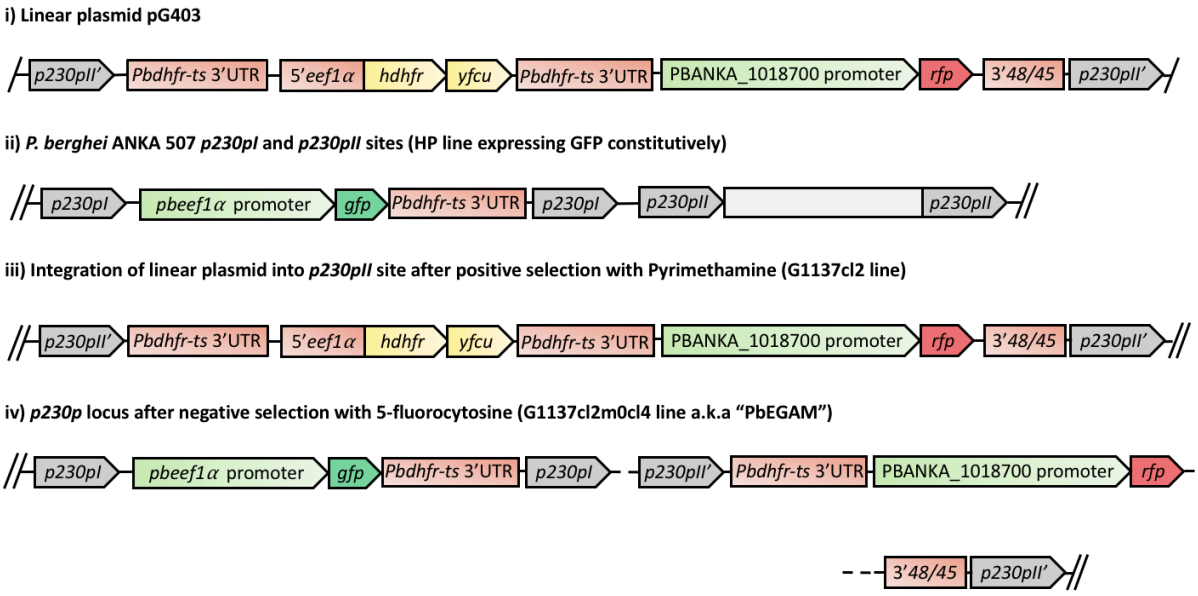

Supplemental Image 1B: The *P. berghei* ANKA "early gametocyte" ("PbEGAM") background line. In **i)** is the linearised pG403 plasmid, in which an *rfp* sequence is driven by the promoter of a recently identified genetic marker for early gametocytogenesis (RFP signal at 8-12 hpi), PBANKA_1018700 (Sinha *et al.*, 2014; Rebecca S. Lee, Waters and Brewer, 2018). In this plasmid, both drug selection and fluorescent cassettes are flanked by sequences homologous to a second site of the *p230p* locus: *p230pII*. Between these homology arms are the *hdhfr::yfcu* positive/negative drug selectable markers, driven by the *5'eef1α* promoter, and flanked by two identical *pbdhfr-ts* 3'UTRs. The *PBANKA_1018700 promoter::rfp* fluorescent cassette is contained between two non-identical 3'UTRs: the first being the second *pbdhfr-ts* 3'UTR of the drug selectable cassette, with a *3'48/45* UTR located downstream of *rfp*. This DNA construct was designed so as to be inserted into the *p230p* locus of the *P. berghei* ANKA 507 background line shown in **ii)**, a line in which GFP is constitutively expressed throughout the life cycle (Janse, Ramesar and Waters, 2006). In **ii),** the *p230pI* and *p230pII* sites of the *P. berghei* 507 line are shown. The *p230pII* site is akin to WT *P. berghei* ANKA, while the *p230pI* site contains a GFP reporter sequence (*gfp*) that is driven by the constitutively-expressed *pbeef1α* promoter, and flanked downstream by a *pbdhfr-ts* 3'UTR. **iii)** shows the 507 *p230pII* site after integration of the linear plasmid (**i**), but before negative selection (creating *P. berghei* ANKA line G1137cl2). In **iv)**, the full *p230pI* and *p230pII* sites are shown as they would appear after negative selection with 5-FC, and after the drug selection cassette has been removed by recombination.

i) Linear plasmid pG230

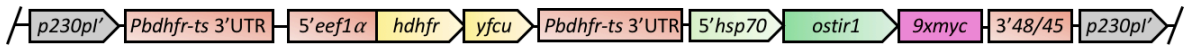

ii) *P. berghei* ANKA high-producer (HP) *p230p*l locus

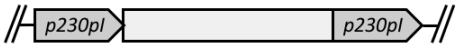

iii) Integration of linear plasmid after positive selection with Pyrimethamine (G615cl1 line)

iv) *p230p* locus after negative selection with 5-fluorocytosine (G615cl1m1cl1 line a.k.a "AID" background line)

Supplemental Image 1C: The *P. berghei* ANKA auxin-inducible degron ("AID") background line. In **i)**, linearised plasmid pG230 is depicted. This plasmid is designed for integration into the *p230pl* site of the *P. berghei* HP line genome. Two *p230p'* homology arms flank a *5'eef1α* promoter-driven *hdhfr::yfcu* cassette (again flanked by identical *pbdhfr-ts* 3'UTRs), and a DNA sequence containing the 'F-box' transport inhibitor response protein 1 (TIR1*)* gene sequence from *Oryza sativa (ostir1*) (Philip and Waters, 2015). This *ostir1* sequence is driven by a potent, constitutive promoter of *P. berghei* heat shock protein 70 *(5'hsp70)* (PBANKA_0711900) (Manzoni *et al.*, 2015). The *ostir1* sequence is also bound to 9 repeats of the human c-myc tag (EQKLISEEDL) (*9xmyc*) and, further downstream, to a p48/45 3'UTR (*3'48/45*). **ii)** and **iii)** depict the *p230pl* locus of the *P. berghei* ANKA HP clonal line before and after integration of the linearised plasmid. **iii)** also depicts the *p230pl* site as it would appear in parasites after positive selection with Pyrimethamine (line G615cl1). In **iv),** the *p230p* locus of the "AID" background line is shown after negative drug selection with 5-FC. In this clonal line, the *ostir1::9xmyc* sequence is constitutively expressed throughout the *P. berghei* life cycle, enabling conditional degradation of AID-tagged proteins.

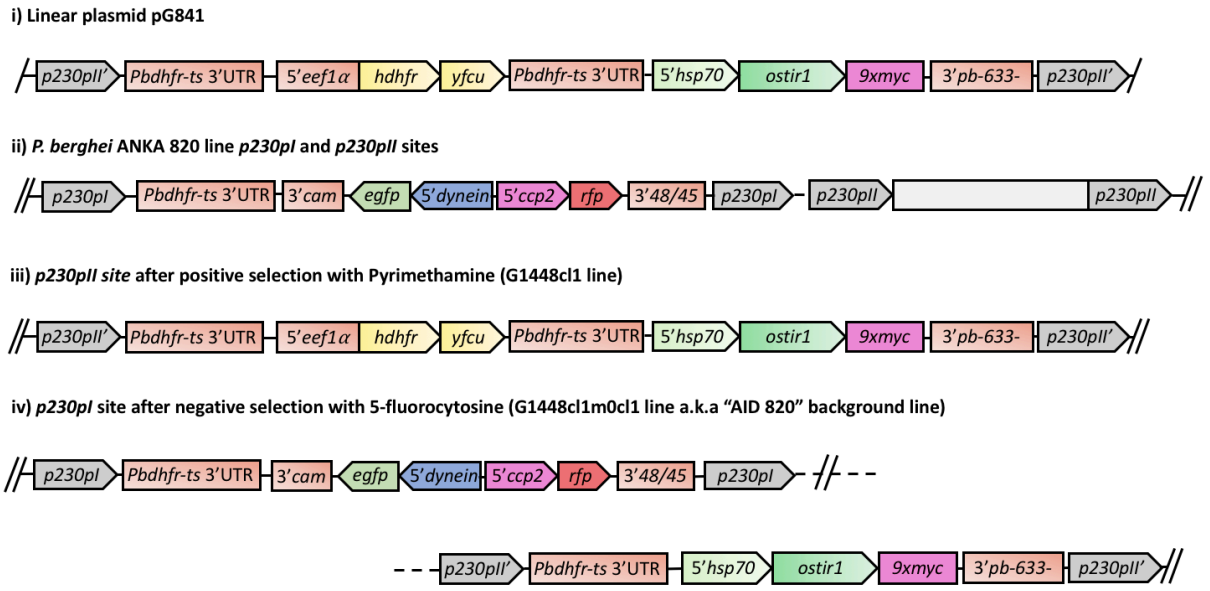

Supplemental Image 1D: The *P. berghei* ANKA "AID 820" background line. Using a near-identical plasmid to that shown in **S3 i),** the AID 820 background line was designed so as to allow both conditional degradation and the ability to monitor male and female gametocytogenesis simultaneously in *P. berghei* ANKA. In **i)**, linearised plasmid pG841 is shown, with homology arms designed for integration of the DNA construct into the *p230pII* site of the 820 background line. This plasmid contains the previously shown *hdhfr::yfcu* drug selection cassette, with a downstream *ostir1::9xmyc* fusion gene that is driven by a *5'hsp70* promoter for constitutive expression. At the 3' end of this fused sequence is the 3'UTR of PBANKA_1318600 (*3' pb-633-*), a previously unused 3' UTR in the AID or 820 background lines (Braks *et al.*, 2008). Usage of this 3'UTR prevented unwanted recombination with other sequences to be integrated into the *P. berghei* ANKA genome. To make this background line, the pG841 linearised plasmid (**i**) was transfected into the 820 background line. **ii)** depicts both the *p230pI* and *p230pII* sites of the "WT" 820 background line. **iii)** shows the *p230pII* site after integration of pG841 and positive drug selection with Pyrimethamine (creating line G1448cl1). In **iv),** the final conformation of the *p230pI* and *p230pII* sites after negative drug selection with 5-FC is shown, creating line G1448cl1m0cl1 (the "AID 820" line) after cloning by limiting dilution.

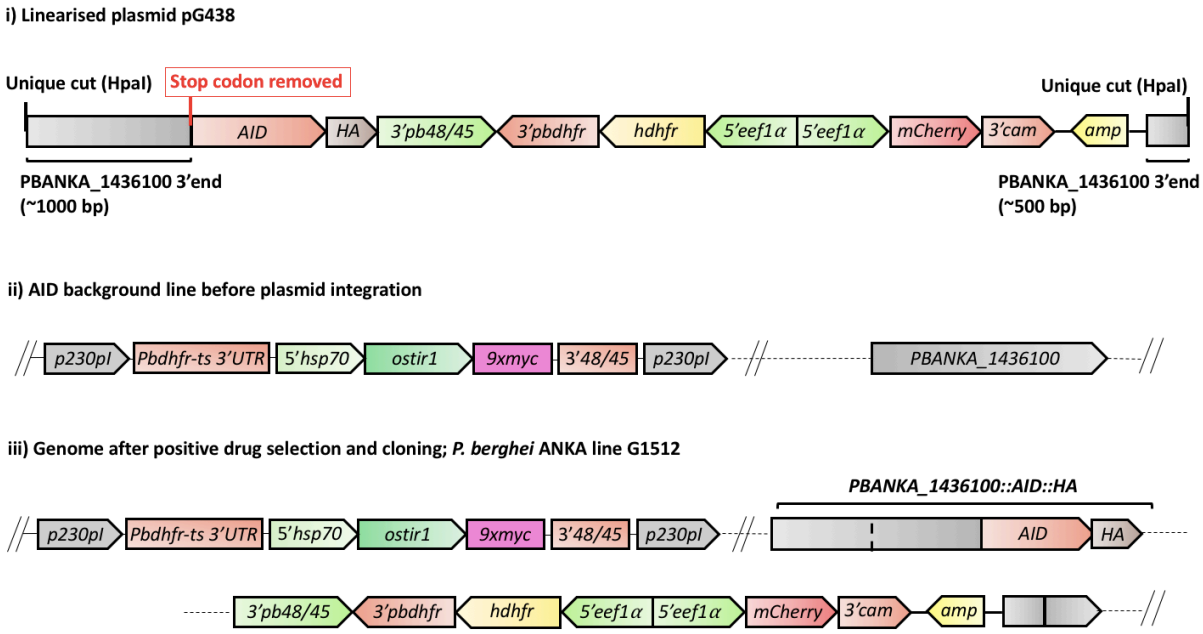

Supplemental Image 1E: *P. berghei* ANKA line G1512: AID-tagged heterochromatin protein 1 (HP1). i) shows linearised plasmid pG438, designed for single-crossover homologous recombination with the endogenous *P. berghei* ANKA HP1 sequence (PBANKA_1436100) (Carvalho and Ménard, 2005). A sequence of ~1500 bp of the HP1 gene (and some upstream sequence) was inserted into an AID-containing background plasmid (pG364), upstream of an *AID::HA* tag. The final stop codon of the gene-of-interest (GOI) coding sequence (TAG, TAA, or TGA) was removed. A 3'UTR of the *P. berghei* ANKA p48/45 gene (*3'pb48/45*) was placed downstream of the *AID::HA* tag. Downstream of this tagging sequence, a bidirectional *P. berghei eef1α* promoter controls both the expression of a positive selection sequence *(hdhfr*, with *pbdhfr* 3'UTR), and a fluorescent mCherry protein (*mCherry*, with a calmodulin gene 3'UTR (*3'cam*)). The pG438 plasmid shown in **i)** is linearised by restriction enzyme digestion with Hpa1, this being because both the HP1 endogenous sequence, and the pG364 plasmid backbone, contain only one Hpa1 restriction site which can cut the plasmid at one unique point to facilitate integration into the *P. berghei* AID background line. **ii)** shows the *p230pI* locus of the AID background line (expressing *ostir1::9xmyc*), and the WT HP1 gene. In **iii)**, both the *p230pI* locus and the AID::HA-tagged HP1 gene are shown as they would appear following positive selection with Pyrimethamine. A residual ampicillin resistance sequence (*amp*) remains in the plasmid backbone after integration. In this case, the *hdhfr* drug selection marker was not removed by negative selection after integration of the plasmid (as a fused *hdhfr::yfcu* cassette was not used).

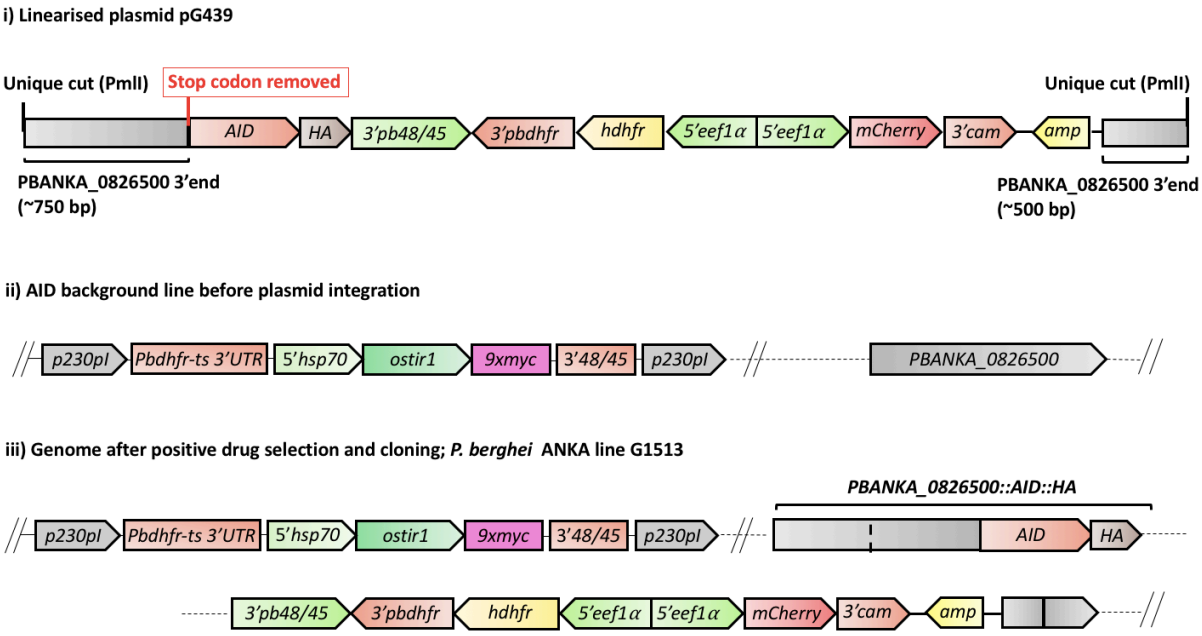

Supplemental Image 1F: *P. berghei* ANKA line G1513: AID-tagged histone deacetylase 1 (HDAC1). **i)** depicts the linearised pG439 single-crossover plasmid. Like pG438 (**S1E i)**), the pG364 background vector containing a *hdhfr* positive drug selection cassette and *P. berghei eef1α* promoter-driven mCherry tag was used, though in this case, the HDAC1 protein (PBANKA_0826500) was tagged at the 3' end with the AID::HA fused protein. In this case, the circular plasmid was linearised by restriction digest with PmlI, leaving an approximate 750 bp fragment (without stop codon) to integrate into the WT HDAC1 protein by single-crossover homologous recombination. In **ii),** the AID background line *p230pI* site is shown, located upstream of the WT HDAC1 gene (PBANKA_0826500). After transfection and positive drug selection, the final AID-tagged HDAC1 line would appear as in **iii)** (*P. berghei* ANKA line G1513.

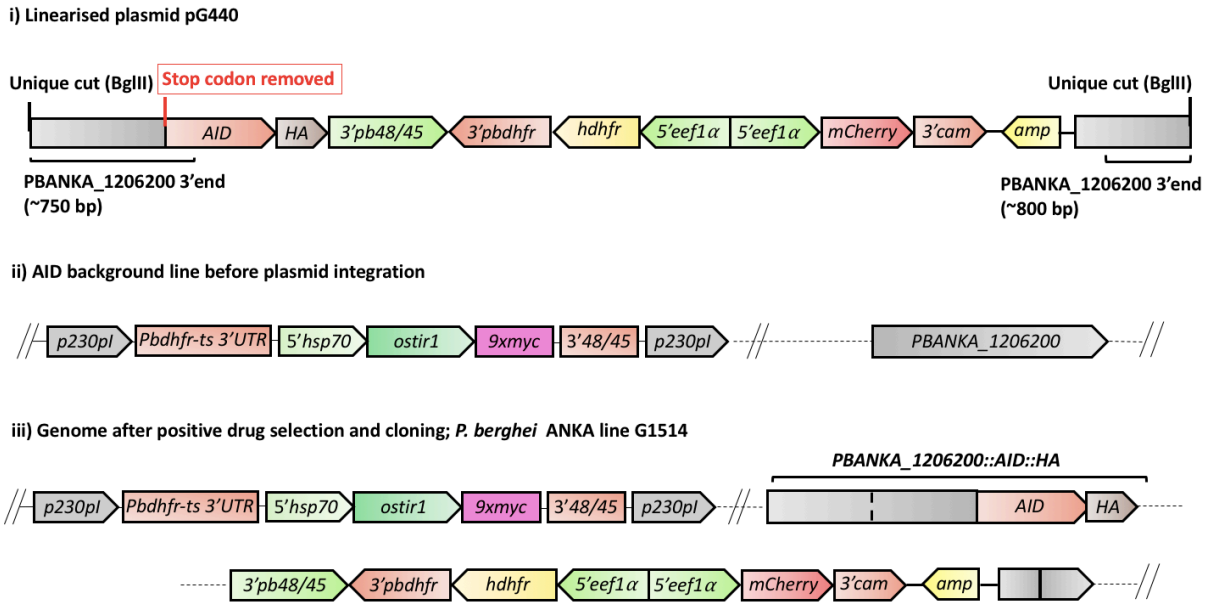

Supplemental Image 1G: *P. berghei* ANKA line G1514: AID-tagged histone deacetylase 2/inositol phosphate kinase 1 (HDAC2/IPK1). i) is a diagrammatic representation of the linearised pG440 plasmid (not to scale), showing an adaptation of the pG364 background vector to tag the whole HDAC2/IPK1 (a fused protein; PBANKA_1206200) with an AID::HA tag at its C-terminus. As is necessary for C-terminal tagging, the HDAC2/IPK1 stop codon has been removed and, in this case, the unique restriction site for BglII was used to linearise the DNA construct. **ii)** depicts the *ostir1::9xmyc*-expressing sequence at the *p230pI* site, with the WT PBANKA_1206200 located downstream. In **iii),** the final, positively-selected *P. berghei* ANKA G1514 line is shown, with *ostir::9xmyc* expressed at the *p230pI* locus and the HDAC2/IPK1 protein tagged with AID::HA. G1514 parasites can be drug-selected (*eef1α* promoter-driven *hdhfr* sequence) or separated by FACS based on mCherry fluorescence (*eef1α* promoter-driven *mcherry* sequence).

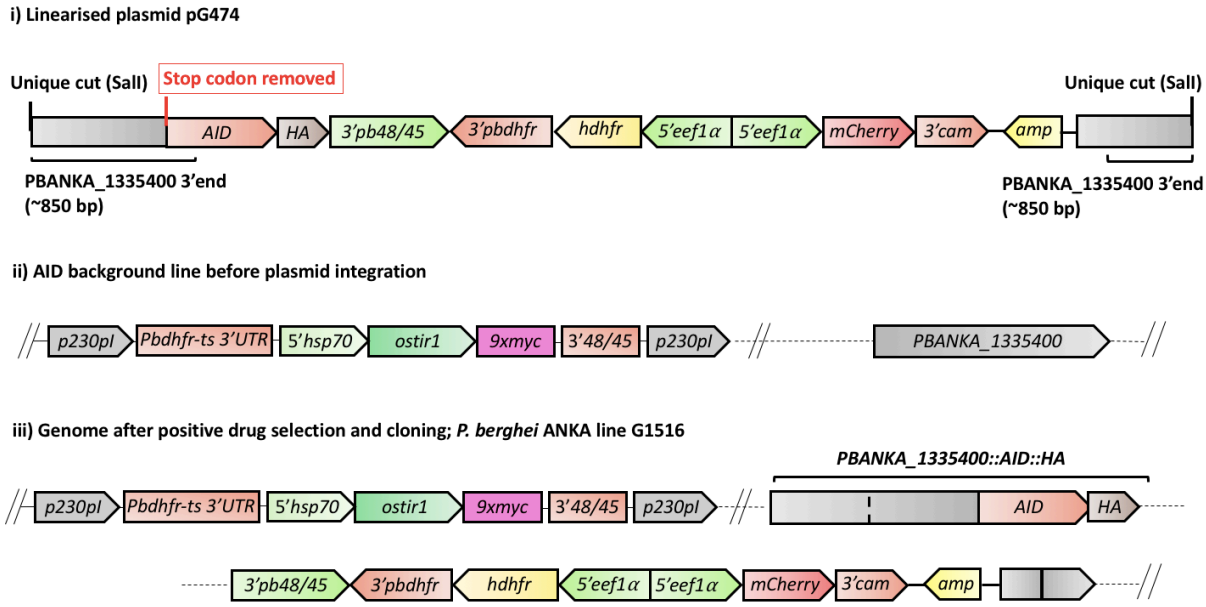

Supplemental Image 1H: *P. berghei* ANKA line G1516: an AID-tagged histone deacetylase 1 (HDA1). i) depicts the linearised pG474 plasmid vector for the C-terminal tagging of HDA1 (PBANKA_1335400) with an AID:HA fused tag. In the absence of an endogenous unique restriction site within the HDA1 sequence, a SalI restriction site was added during amplification of the HDA1 homology arms by PCR. Restriction digest with SalI produced a linearised pG474 plasmid with two homologous sequences of ~850 bp at either side of the single-crossover cassette (the pG364 background plasmid once more). As usual, the final HDA1 stop codon was removed. In **ii),** the *p230pI* site of the AID background parasite line is shown, with the WT HDA1 gene located downstream (PBANKA_1335400). **iii)** depicts the final *p230pI* site and AID::HA-tagged HDA1 gene, creating the *P. berghei* ANKA G1516 line after positive selection with Pyrimethamine.

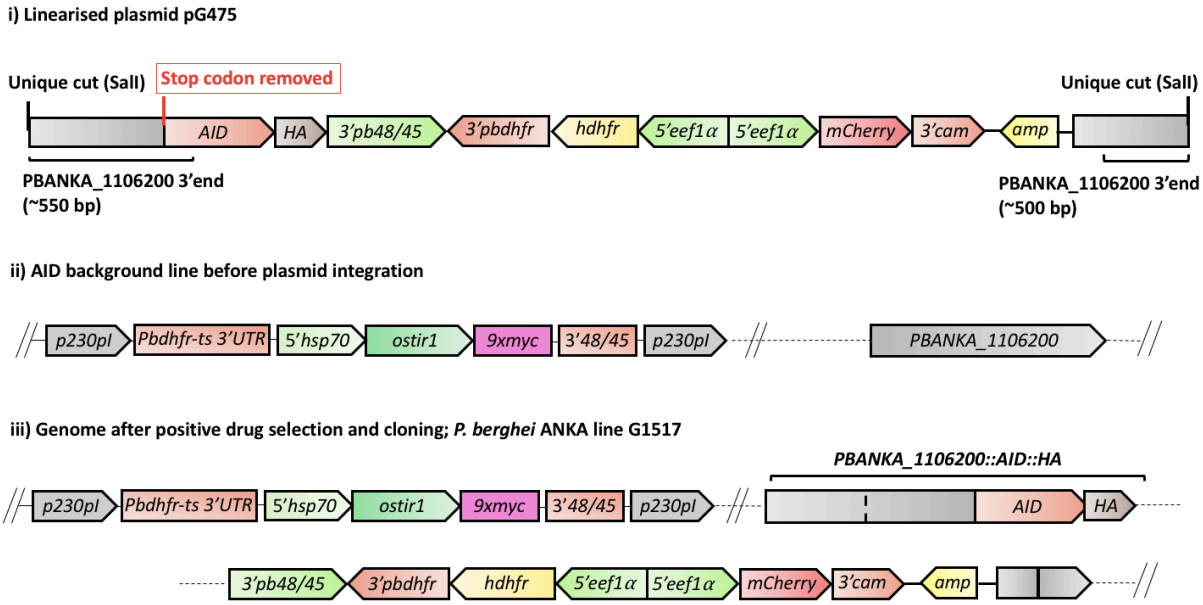

Supplemental Image 1I: *P. berghei* ANKA line G1517: an AID-tagged putative histone deacetylase (HDA, putative, a.k.a "HDAP"). i) shows the linearised pG475 plasmid, based on the AID::HA tagging vector, pG364. In this case, as in the case of HDA1 (**S1H**), a SalI restriction site was inserted into the HDAP sequence during amplification of homology arms for single-crossover homologous recombination. The stop codon of HDAP was removed and so the *AID::HA* sequence is translated at the C-terminus of HDAP. A bidirectional *eef1α* promoter again drives both a *hdhfr* sequence, and an *mCherry* sequence for isolation and selection of the successfully-tagged *P. berghei* parasites. In **ii),** the *p230pl* site of the *P. berghei* AID background line is depicted with the WT HDAP sequence shown downstream (PBANKA_1106200). The final, positively-selected parasites (named *P. berghei* ANKA line G1517) have a *p230pl* site and AID::HA-tagged HDAP gene as depicted in **iii).**

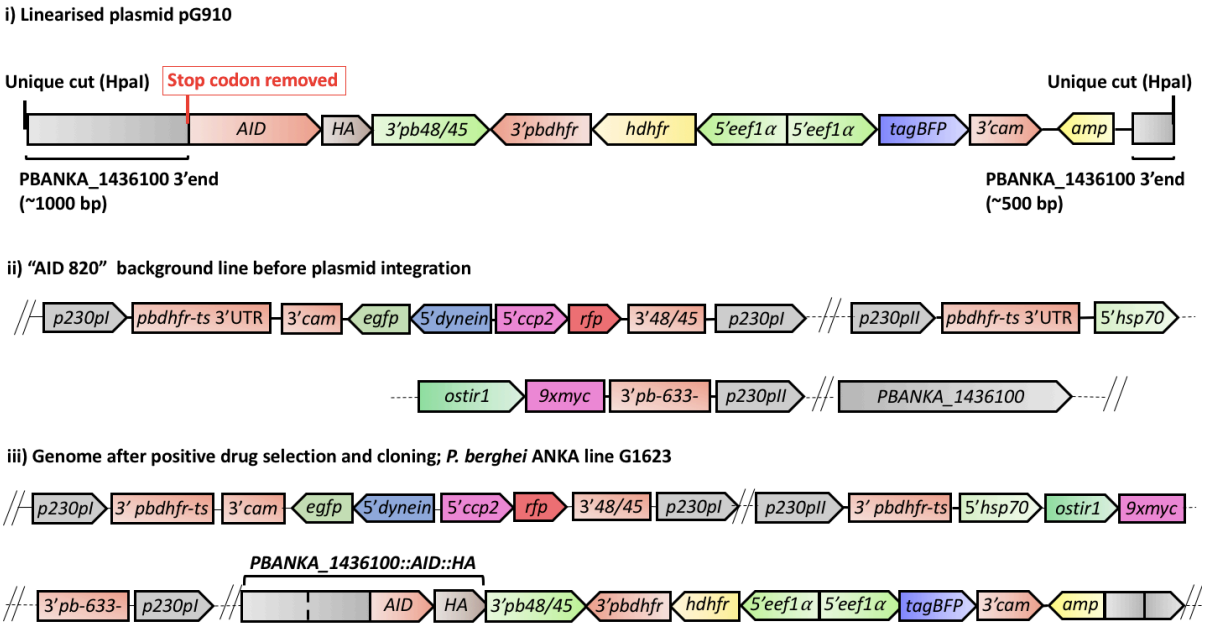

Supplemental Image 1J: *P. berghei* ANKA line G1623: AID- and BFP- tagged heterochromatin protein 1 (HP1). i) depicts the linearised pG910 plasmid, an AID::HA-tagging vector for the HP1 gene of *P. berghei* ANKA. Unlike the AID::HA-tagging plasmid shown in **S1E i)**, this plasmid was made using the background *tagBFP*-containing vector, pG472. In this case, HP1 was uniquely cut again by Hpa1 restriction digest, and the stop codon of the HP1 gene sequence had been removed for expression of the AID::HA tag at the HP1 C-terminus. In the plasmid, pG910, a bidirectional *eef1α* promoter drives a *hdhfr* sequence (to enable positive drug selection with Pyrimethamine), and the *tagBFP* sequence with a *P. berghei* ANKA calmodulin 3'UTR (*3'cam*). This linearised plasmid was then transfected into the 820 *P. berghei* background line, the *p230pI* and *p230pII* sites of which is shown in **ii).** The WT HP1 gene (PBANKA_1436100) is shown downstream of the GFP/RFP-containing locus (as the *p230p* locus is located on chromosome 3 (of 14) in the *P. berghei* genome (PBANKA_0306000)). In **iii),** the final G1623 line is shown after positive selection with Pyrimethamine. The male gametocyte-specific heavy dynein chain (PBANKA_0416100) promoter drives *egfp* expression. The promoter of the female gametocyte-specific LCCL-domain containing gene, Ccp2 (*ccp2*) (PBANKA_1319500) drives the red fluorescent protein sequence (*rfp*), and the integration of the AID::HA-tagged HP1 vector should produce constitutive expression of the blue fluorescent protein (BFP) reporter sequence (*tagBFP*). The *eef1α* promoter sequence also drives the *hdhfr* positive drug selection sequence, with *ostir1::9xmyc* constitutively expressed at the *p230pII* site.

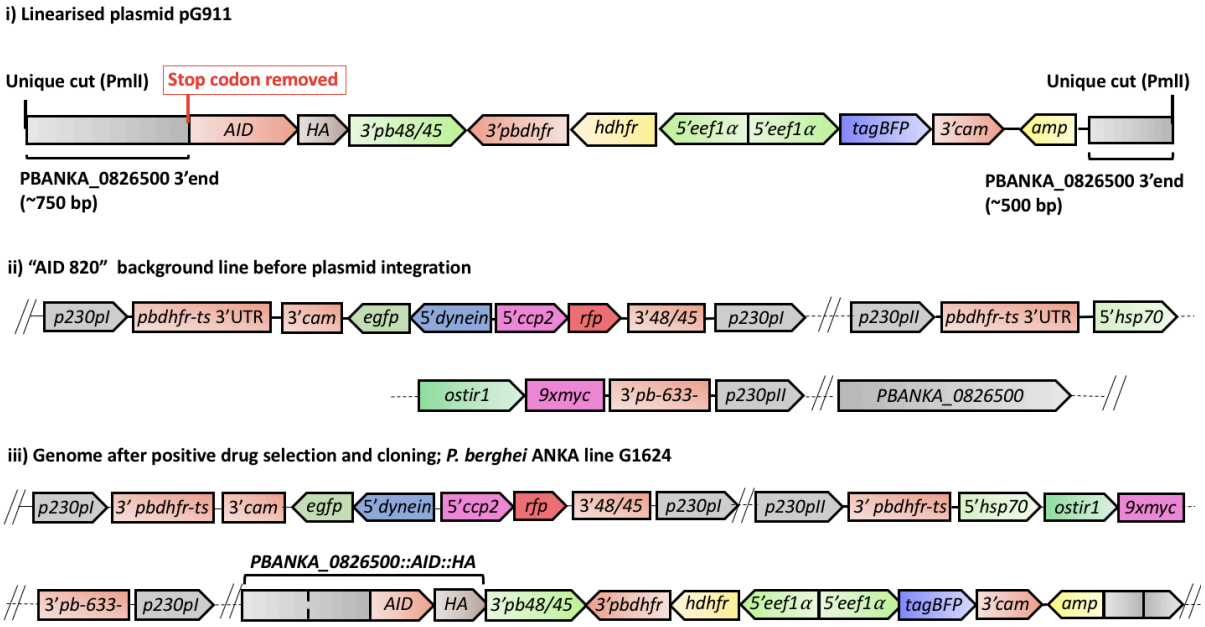

Supplemental Image 1K: *P. berghei* ANKA line G1624: AID- and BFP- tagged histone deacetylase 1 (HDAC1). i) depicts the linearised pG911 plasmid which differs from that of the pG439 plasmid shown in **S1F i)** at the fluorescent reporter sequence. Using the pG472 background plasmid, pG911 was made so that *P. berghei* parasites containing an AID::HA-tagged HDAC1 protein will exhibit BFP fluorescence in background parasites that already contain the male and female gametocyte-specific GFP/RFP expression cassette. In **ii),** the *p230pI* and *p230pII* sites of the "AID 820" line are shown, positioned upstream of the WT HDAC1 gene. Upon integration of the plasmid and positive drug selection with Pyrimethamine, the new G1624 parasites contain the background sequences as shown in **iii).** This line could then be used to monitor the effect of HDAC1 conditional degradation on male and female gametocytes separately.

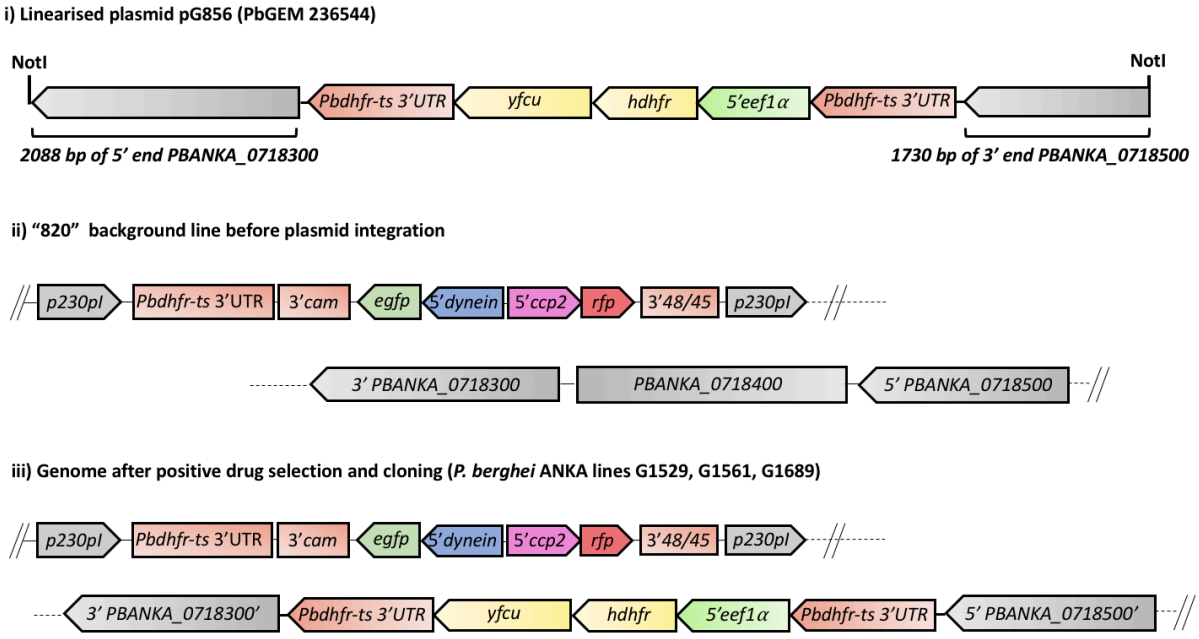

Supplemental Image 1L: Histone acetyltransferase 1 (HAT1) knockout in the *P. berghei* ANKA 820 line. Unlike plasmids used to tag GOIs by single-crossover homologous recombination, gene knockout plasmids obtained from the *Plasmo*GEM database (Schwach *et al.*, 2015) contain long homology arms to replace a GOI with a *hdhfr::yfcu* drug selection cassette. **i)** shows the linearised pG856 plasmid (PbGEM 236544) after restriction digest with NotI. All *Plasmo*GEM DNA constructs are bacteriophage N15-based pJAZZ OK vectors that are linearised at a NotI restriction site (Pfander *et al.*, 2013). To target the HAT1 gene (PBANKA_0718400), a *hdhfr::yfcu* drug selection cassette (driven by a *5'eef1α* promoter and flanked by identical *pbdhfr-ts* 3'UTRs) is placed between a 2088 bp region of the upstream gene (PBANKA_0718300) and a 1730 bp sequence homologous to the downstream gene (PBANKA_0718500). In **ii),** the *p230pI* site and WT HAT1 gene are depicted as they would be in the "WT" 820 line prior to integration of the pG856 plasmid. **iii)** then shows the *p230pI* site and the GOI (HAT1) site as it would appear after positive drug selection and cloning. For the purposes of the present study, negative selection with 5-FC to remove the *hdhfr::yfcu* cassette was not necessary.

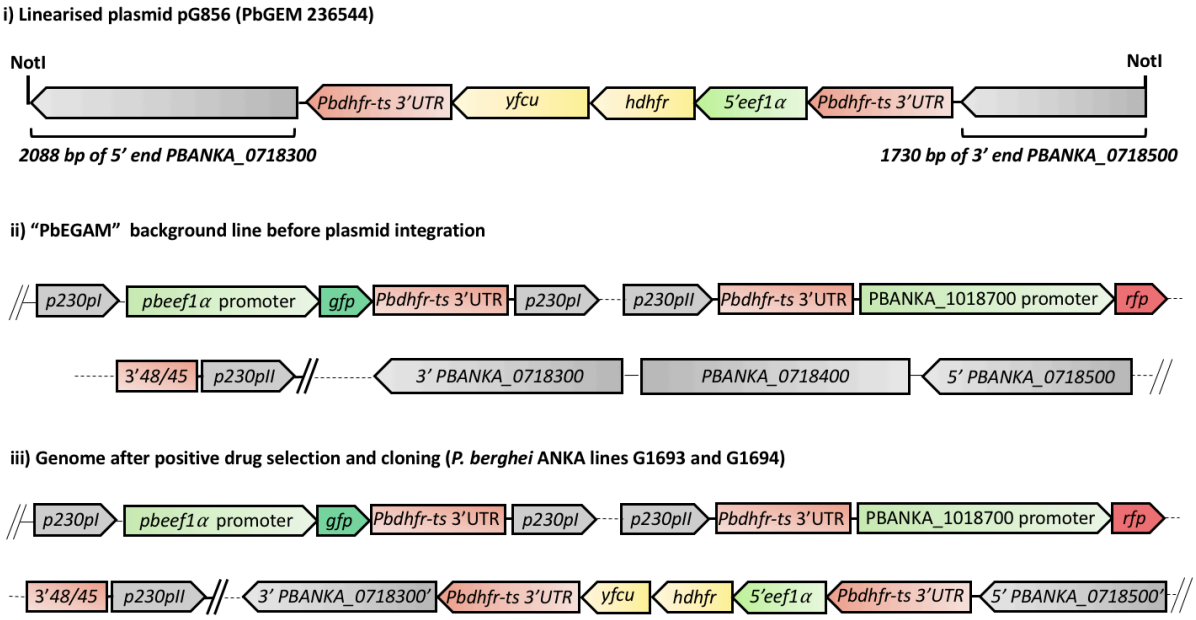

Supplemental Image 1M: Histone acetyltransferase 1 (HAT1) knockout in the *P. berghei* ANKA PbEGAM line. As in **S1L,** the pG856 *Plasmo*GEM knockout vector was used to replace the HAT1 gene with a *hdhfr::yfcu* drug-selectable cassette (**i**). In this case, the linearised pG856 plasmid was transfected into the PbEGAM "early gametocyte" *P. berghei* ANKA line, depicted in **ii).** In **ii)**, the *p230pI* and *p230pII* integration sites of the *p230p* locus are shown. In *p230pI*, a constitutive *pbeef1α* promoter drives a *gfp* fluorescent reporter sequence (with a *pbdhfr-ts* 3'UTR). At the adjacent, downstream *p230pII* site, an *rfp* sequence is driven by the PBANKA_1018700 promoter (with fluorescence in gametocytes seen from 8-12 hpi) (Rebecca S Lee, Waters and Brewer, 2018). Further downstream again is the HAT1 gene (PBANKA_0718400). The nearest upstream and downstream genes are also depicted as the homology arms of the *Plasmo*GEM vector span these regions. Following transfection of the linearised plasmid and positive drug selection, the final *p230p* locus and HAT1 region of the *P. berghei* genome is arranged as in **iii).** As with other KO experiments in this study, negative drug selection was not required for these KO lines.

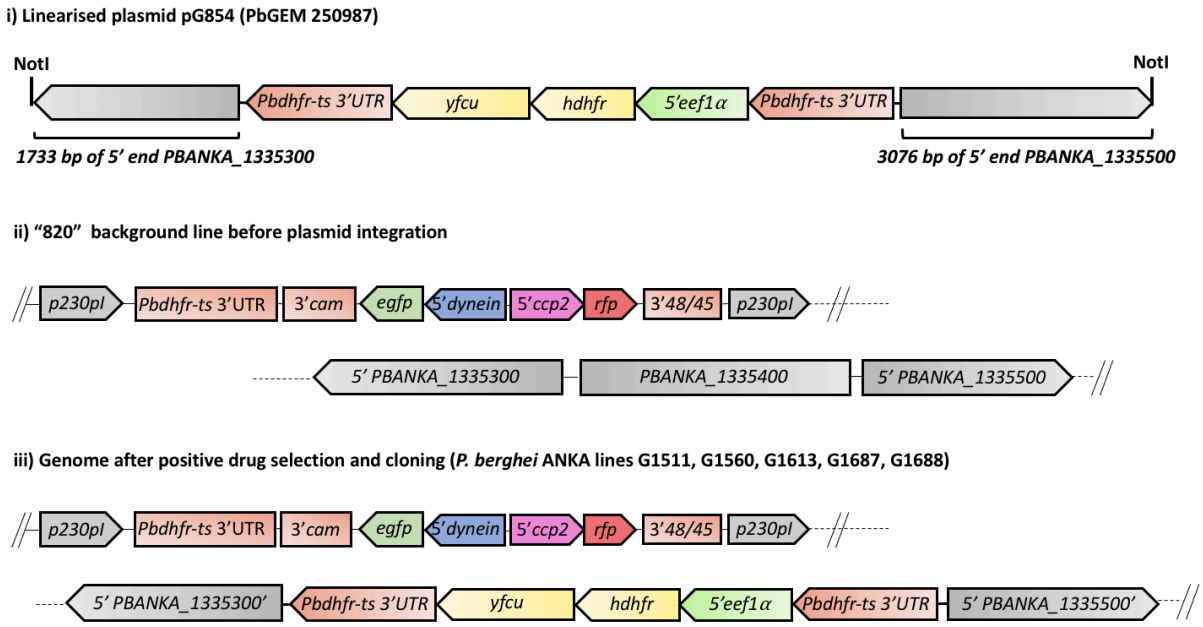

Supplemental Image 1N: Histone deacetylase 1 (HDA1) knockout in the *P. berghei* ANKA 820 line. As in **S1L,** knockout (KO) of putative histone deacetylase 1 (HDA1) (PBANKA_1335300) was undertaken using a *Plasmo*GEM vector. In **i),** HDA1 KO plasmid pG854 (PbGEM 250987) is depicted. As was the case with the HAT1 KO plasmid, the long homology arms of pG854 encompass 1733 bp of the upstream gene (PBANKA_1335300) and 3076 bp of the downstream gene (PBANKA_1335500) to facilitate double-crossover homologous recombination with the WT HDA1 gene. When integrated into the background *P. berghei* ANKA line, the HDA1 coding region is replaced by a *hdhfr::yfcu* drug selection cassette. **ii)** shows the *p230pI* site and the "WT" HDA1 locus of the 820 line before transfection. In **iii),** the linearised pG854 has been integrated into the 820 genome and positive drug selection with Pyrimethamine carried out, leaving behind the GFP/RFP male/female gametocyte fluorescent reporters at *p230pI* and a *hdhfr::yfcu* cassette in place of the HDA1 gene.

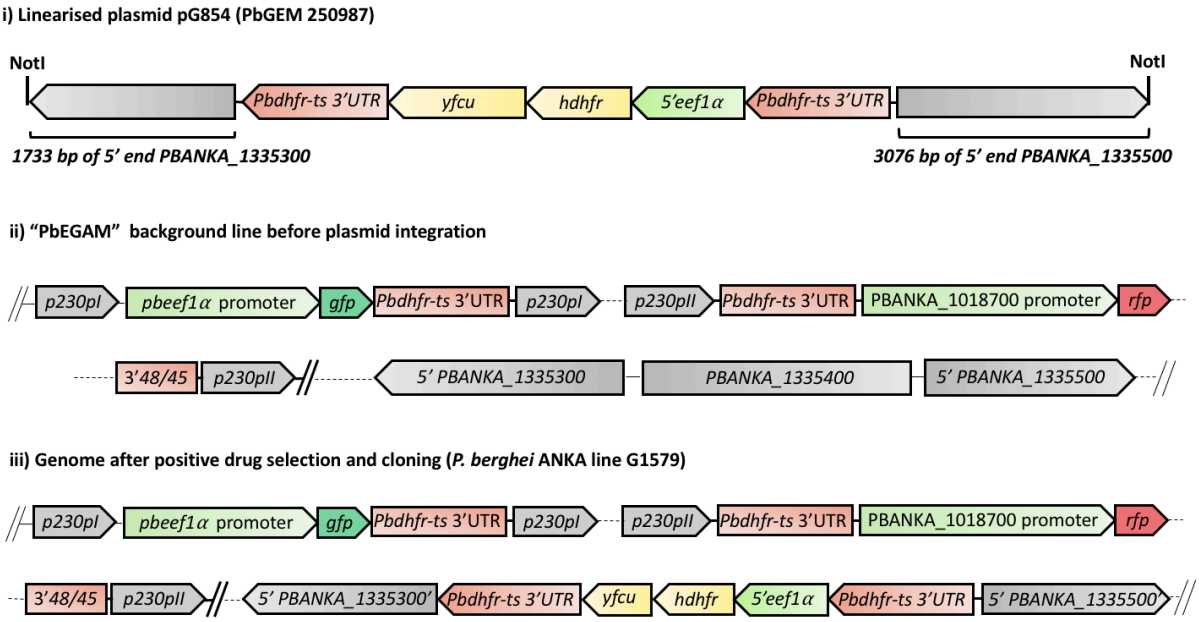

Supplemental Image 1O: Histone deacetylase 1 (HDA1) knockout in the *P. berghei* ANKA PbEGAM line. As in **S1N,** the pG854 *Plasmo*GEM vector was used for the knockout (KO) of HDA1 by double-crossover homologous recombination (**i**). In **ii),** the *P. berghei* ANKA PbEGAM *p230pI* and *p230pII* sites of the *p230p* integration locus are shown, with the HDA1 gene and adjacent genes depicted downstream. Following transfection of the NotI-cut, linearised pG854 plasmid and positive drug selection, the *p230p* locus and HDA1 locus appear as depicted in **iii).** In the resultant line (G1579), no negative selection was necessary as no further genetic manipulation of the parasite line was warranted in this study.

Supplemental Section S1

S1.1 The histone 4 (H4) of *P. berghei*

Of all eukaryotic histone types and variants, histone 4 (H4) is most conserved (Malik and Henikoff, 2003), and this conservation of the H4 sequence remains in *Plasmodium spp.* (**Figure S1**). Using a combination of Clustal multiple sequence alignment (Sievers and Higgins, 2014) and basic local alignment search tool (BLAST) for protein sequences (blastp) (Altschul *et al.*, 1990), the *P. berghei* ANKA H4 peptide sequence was compared to those of four available human-infective *Plasmodium* species (*P. vivax, P. knowlesi, P. malariae,* and *P. falciparum*) alongside H4 amino acid sequences from the mouse (*Mus musculus*), rat (*Rattus norvegicus*), and human (*Homo sapiens sapiens*) (**Figure S1).** As can be seen in **Figure S1**, the amino acid sequences of all *Plasmodium spp.* are identical. Between *Plasmodium spp.* and mammals, the majority of amino acids are also conserved, with all but two amino acid changes being between residues with strongly similar physiochemical properties (based on a PAM (partitioning around medoids) 250 matrix scoring system of protein similarity (Gonnet, Cohen and Benner, 1992; Pearson, 2013)). Furthermore, each H4 sequence is exactly 103 amino acids (aa) in length.

Taking *P. berghei* ANKA H4 as a reference, protein-protein blastp alignment revealed 92% sequence identity to the H4 sequences of *M. musculus, R. norvegicus,* and *H. sapiens sapiens* (blastp alignments not shown). In fact, all mammalian H4 sequences were identical.

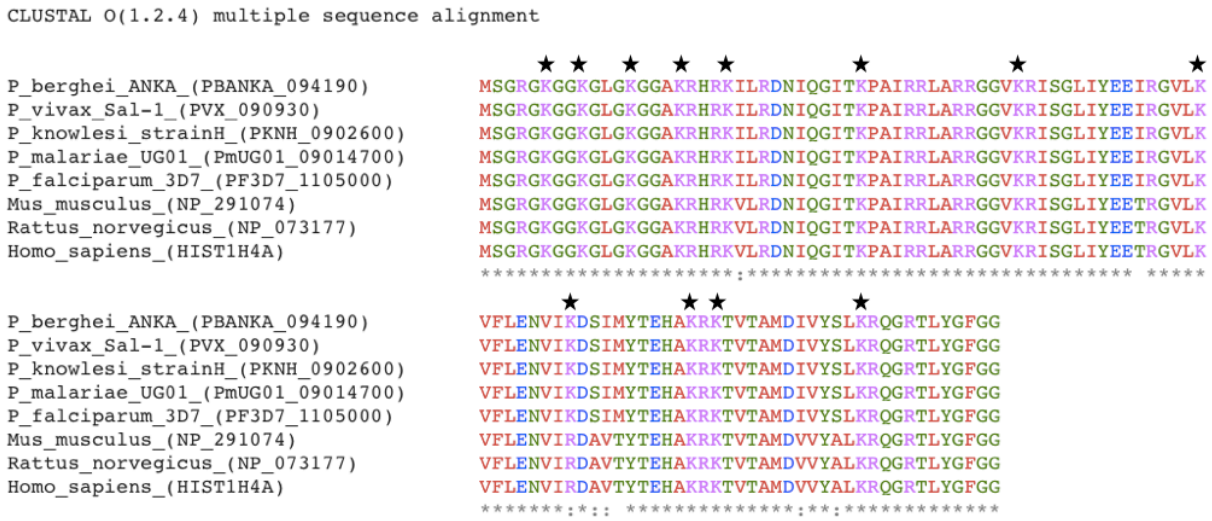

Figure S1: Clustal alignment of *Plasmodium spp*. histone 4 (H4). The above alignment of histone 4 amino acid sequences was carried out using Clustal Omega (Sievers and Higgins, 2014) and shows a comparison of histone 4 peptide sequences from *P. berghei* ANKA, *P. vivax* isolate Salvador 1 (Sal-1), *P. knowlesi* macaque-adapted experimental strain H, *P. malariae* Uganda 01 (UG01) isolate, *P. falciparum* strain 3D7, the mouse *Mus musculus*, the rat *Rattus norvegicus* strain, and *Homo sapiens sapiens* (*P. ovale curtisi/wallikeri* H4 sequence data unavailable at time of writing [07-02-18]). Peptides are distinguished from one another by colour, and the positions of lysines (often the target for post-translational modifications) are further indicated by a star (★) above their amino acid letter (K). In Clustal, an asterisk (*) below an aligned amino acid indicates that the amino acid is fully conserved. A colon (:) underneath an aligned amino acid indicates conservation between residues with strongly similar properties (scoring an equivalent of >0.5 the Gonnet PAM 250 matrix (Pearson, 2013)). A full stop/period (.) below an aligned amino acid indicates conservation of residues with weakly similar properties (roughly equivalent to a score of >0 but <0.5 on the Gonnet PAM 250 matrix (Pearson, 2013)). No symbol beneath an aligned amino acid signifies that there is no conservation of the amino acid or exchange for an amino acid with similar properties.

S1.2 The canonical histone 3 (H3) of *P. berghei*

In mammals, two canonical, non-centromeric H3 histones are expressed (designated H3.1 and H3.2) and differ in their binding partners during DNA synthesis (Latreille *et al.*, 2014; Maehara *et al.*, 2015). At the amino acid level, all H3.1 and H3.2 peptides are 136 aa in length, with the H3.1 and H3.2 sequences differing at only one point. At position 96 of the 136 aa sequence (not counting the first methionine), H3.2 contains a serine, with the H3.1 sequence containing a cysteine at the same position (**Figure S2 (A)**). **Figure S2 (A)** shows a Clustal alignment of the human H3.1 and H3.2

protein sequences, though this same amino acid substitution is conserved between H3.1 and H3.2 sequences of both *M. musculus* (protein accessions P68433.2 (H31_MOUSE) and P84228.2 (H32_MOUSE)) and *R. norvegicus* (protein accessions Q6LED0.3 (H31_RAT) and D3Z80J (D3Z80J_RAT)) (all alignments not shown).

In *P. berghei* ANKA, only one canonical histone 3 (H3) is present (encoded for by PBANKA_0108800) and it shows 93% sequence identity to both the H3.1 and H3.2 protein sequences of mammalian H3, with blastp total scores differing by one digit (total blastp scores were 260 and 259 for H3.2 and H3.1 respectively) (blastp results not shown). As a result of an overall higher total score, *Plasmodium spp.* sequences were aligned to the mammalian H3.2 protein sequences (**Figure S2 (B)**).

In *P. berghei* ANKA, at position 96 (the position that defines H3.1 and H3.2), the serine(S) and cysteine (C) residues are replaced by an alanine (A), a change that is conserved among all *Plasmodium spp.* Taking all *Plasmodium* H3 protein sequences alone, only one of the six aligned sequences showed a deviation from the others (**Figure S2 (B)**). Though the H3 sequences of *P. berghei, P. falciparum, P. vivax, P. ovale curtisi,* and *P. malariae* were 100% identical, the canonical H3 of *P. knowlesi* strain H showed a number of amino acid substitutions, with 94% sequence identity to the other *Plasmodium spp.* overall (blastp results not shown). The changes to the canonical *P. knowlesi* H3 are often between amino acids that share similar physiochemical properties, though it should be noted that among these changes is the substitution of an arginine (R) to a lysine (K) at position 53, a change that may have downstream post-translational consequences. Notably, R53 is conserved between all mammalian and *Plasmodium spp.* H3 sequences, with *P. knowlesi* GH01 being the only outlier (**Figure S2 (B)**).

A

```
CLUSTAL O(1.2.4) multiple sequence alignment


sp|P68431|H31_HUMAN       MARTKQTARKSTGGKAPRKQLATKAARKSAPATGGVKKPHRYRPGTVALREIRRYQKSTE
sp|Q71DI3|H32_HUMAN       MARTKQTARKSTGGKAPRKQLATKAARKSAPATGGVKKPHRYRPGTVALREIRRYQKSTE
                          ************************************************************

sp|P68431|H31_HUMAN       LLIRKLPFQRLVREIAQDFKTDLRFQSSAVMALQEACEAYLVGLFEDTNLCAIHAKRVTI
sp|Q71DI3|H32_HUMAN       LLIRKLPFQRLVREIAQDFKTDLRFQSSAVMALQEASEAYLVGLFEDTNLCAIHAKRVTI
                          ************************************.***********************

sp|P68431|H31_HUMAN       MPKDIQLARRIRGERA
sp|Q71DI3|H32_HUMAN       MPKDIQLARRIRGERA
                          ****************
```

B

```
CLUSTAL O(1.2.4) multiple sequence alignment


                                    *  *  *  *  *  *     **                 *
Mus_musculus_histone3.2_(NP_038576)          MARTKQTARKSTGGKAPRKQLATKAARKSAPATGGVKKPHRYRPGTVALREIRRYQKSTE
Rattus_norvegicus_histone3c2_(NP_001101168)  MARTKQTARKSTGGKAPRKQLATKAARKSAPATGGVKKPHRYRPGTVALREIRRYQKSTE
Homo_sapiens_(HIST2H3A)                      MARTKQTARKSTGGKAPRKQLATKAARKSAPATGGVKKPHRYRPGTVALREIRRYQKSTE
P_berghei_ANKA_(PBANKA_010880)               MARTKQTARKSTAGKAPRKQLASKAARKSAPISAGIKKPHRYRPGTVALREIRRYQKSTD
P_vivax_Sal-1_(PVX_113665)                   MARTKQTARKSTAGKAPRKQLASKAARKSAPISAGIKKPHRYRPGTVALREIRRYQKSTD
P_malariae_UG01_(PmUG01_11052600)            MARTKQTARKSTAGKAPRKQLASKAARKSAPISAGIKKPHRYRPGTVALREIRRYQKSTD
P_ovale_curtisi_GH01_(PocGH01_11046400)      MARTKQTARKSTAGKAPRKQLASKAARKSAPISAGIKKPHRYRPGTVALREIRRYQKSTD
P_falciparum_3D7_(PF3D7_0610400)             MARTKQTARKSTAGKAPRKQLASKAARKSAPISAGIKKPHRYRPGTVALREIRRYQKSTD
P_knowlesi_strainH_(PKNH_1132500)            MARTKQTARKSTGGKAPRKQLASKAARKSAPVSTGIKKPHRYRPGTVALREIRKFQKSTD
                                             ***********.*********:******** : *:*****************::*****:

                                       *           *                          *
Mus_musculus_histone3.2_(NP_038576)          LLIRKLPFQRLVREIAQDFKTDLRFQSSAVMALQEASEAYLVGLFEDTNLCAIHAKRVTI
Rattus_norvegicus_histone3c2_(NP_001101168)  LLIRKLPFQRLVREIAQDFKTDLRFQSSAVMALQEASEAYLVGLFEDTNLCAIHAKRVTI
Homo_sapiens_(HIST2H3A)                      LLIRKLPFQRLVREIAQDFKTDLRFQSSAVMALQEASEAYLVGLFEDTNLCAIHAKRVTI
P_berghei_ANKA_(PBANKA_010880)               LLIRKLPFQRLVREIAQDYKTDLRFQSSAVMALQEAAEAYLVGLFEDTNLCAIHAKRVTI
P_vivax_Sal-1_(PVX_113665)                   LLIRKLPFQRLVREIAQDYKTDLRFQSSAVMALQEAAEAYLVGLFEDTNLCAIHAKRVTI
P_malariae_UG01_(PmUG01_11052600)            LLIRKLPFQRLVREIAQDYKTDLRFQSSAVMALQEAAEAYLVGLFEDTNLCAIHAKRVTI
P_ovale_curtisi_GH01_(PocGH01_11046400)      LLIRKLPFQRLVREIAQDYKTDLRFQSSAVMALQEAAEAYLVGLFEDTNLCAIHAKRVTI
P_falciparum_3D7_(PF3D7_0610400)             LLIRKLPFQRLVREIAQDYKTDLRFQSSAVMALQEAAEAYLVGLFEDTNLCAIHAKRVTI
P_knowlesi_strainH_(PKNH_1132500)            LLIRKLPFQRLVREIAQEYKTDLRFQSQAVLALQEAAEAYLVGLFEDTNLCAIHAKRVTI
                                             ****************::********.**:*****:**********************

                                       *
Mus_musculus_histone3.2_(NP_038576)          MPKDIQLARRIRGERA
Rattus_norvegicus_histone3c2_(NP_001101168)  MPKDIQLARRIRGERA
Homo_sapiens_(HIST2H3A)                      MPKDIQLARRIRGERA
P_berghei_ANKA_(PBANKA_010880)               MPKDIQLARRIRGERS
P_vivax_Sal-1_(PVX_113665)                   MPKDIQLARRIRGERS
P_malariae_UG01_(PmUG01_11052600)            MPKDIQLARRIRGERS
P_ovale_curtisi_GH01_(PocGH01_11046400)      MPKDIQLARRIRGERS
P_falciparum_3D7_(PF3D7_0610400)             MPKDIQLARRIRGERS
P_knowlesi_strainH_(PKNH_1132500)            MPKDIQLARRIRGERS
                                             ***************:
```

Figure S2: Clustal alignment of *Plasmodium spp*. canonical histone 3 (H3). In **(A)** above, Clustal alignment of the human H3.1 and H3.2 protein sequences is shown, with the cysteine (C) to serine (S) substitution clearly indicated by a period (.) beneath the residue of interest. In **(B)** alignment of histone 4 amino acid sequences is shown, as carried out using Clustal Omega (Sievers and Higgins, 2014). The alignment in this case includes comparison of canonical histone 3 peptide sequences from *P. berghei* ANKA, *P. vivax* isolate Salvador 1 (Sal-1), *P. knowlesi* macaque-adapted experimental strain H, *P. malariae* Uganda 01 (UG01) isolate, *P. falciparum* strain 3D7, *P. ovale curtisi* Ghana 01 isolate (Poc GH01), and the H3.2 protein sequences of *M. musculus*, *R. norvegicus*, and *H. sapiens sapiens*. Peptides are distinguished from one another by colour, and the positions of lysines (often the target for post-translational modifications) are further indicated by a star (★) above their amino acid letter (K). In Clustal, an asterisk (*) below an aligned amino acid indicates that the amino acid is fully conserved. A colon (:) underneath an aligned amino acid indicates conservation between

residues with strongly similar properties (scoring an equivalent of >0.5 the Gonnet PAM 250 matrix (Pearson, 2013)). A full stop/period (.) below an aligned amino acid indicates conservation of residues with weakly similar properties (roughly equivalent to a score of >0 but <0.5 on the Gonnet PAM 250 matrix (Pearson, 2013)). No symbol beneath an aligned amino acid signifies that there is no conservation of the amino acid or exchange for an amino acid with similar properties.

It is important to note that during the time of writing, a second *P. knowlesi* sequence became available via PlasmoDB; the *P. knowlesi* Malayan strain Pk1A, for which a canonical histone 3 sequence had been assigned (PKNOH_S130206300) (Lapp *et al.*, 2017). Taking both *P. knowlesi* strain H and *P. knowlesi* Malayan strain Pk1A H3 sequences; and aligning them to the other five H3 sequences shown in **Figure S2 (B)**, a Clustal alignment revealed that genome assembly using long-read Pacific Biosciences (PacBio) technology eliminated all but one amino acid change to the *P. knowlesi* H3 sequence (**Figure S3**). With this new assembly, *P. knowlesi* H3 is identical to the other *Plasmodium spp.* H3 sequences besides a single isoleucine (I) to methionine (M) substitution at position 32 (**Figure S3**).

Figure S3: Realignment of *Plasmodium spp.* canonical histone 3 (H3) to include *P. knowlesi* Malayan strain Pk1A data. The image above shows Clustal alignment of canonical histone 3 peptide sequences from *P. berghei* ANKA, *P. vivax* isolate Salvador 1 (Sal-1), *P. malariae* Uganda 01 (UG01) isolate, *P. falciparum* strain 3D7, *P. ovale curtisi* Ghana 01 isolate (Poc GH01), *P. knowlesi* macaque-adapted experimental strain H, and *P. knowlesi* Malayan strain Pk1A. In this alignment, the similarity of the *P. knowlesi* Malayan strain Pk1A H3 to other *Plasmodium spp.* H3 sequences can be seen. The clear disparity of the canonical H3 sequence of *P. knowlesi* strain H to the other species and the

Malayan isolate suggest that the original genome assembly underlying this protein sequence data may be flawed and that the H3 proteins of all *Plasmodium spp.* may be identical, or almost identical, in reality.

In the above alignment the positions of lysines are indicated by a star (★) above their amino acid letter (K). In Clustal, an asterisk (*) below an aligned amino acid indicates that the amino acid is fully conserved. A colon (:) underneath an aligned amino acid indicates conservation between residues with strongly similar properties (scoring an equivalent of >0.5 the Gonnet PAM 250 matrix (Pearson, 2013)). A full stop/period (.) below an aligned amino acid indicates conservation of residues with weakly similar properties (roughly equivalent to a score of >0 but <0.5 on the Gonnet PAM 250 matrix (Pearson, 2013)). No symbol beneath an aligned amino acid signifies that there is no conservation of the amino acid or exchange for an amino acid with similar properties.

S1.3 The histone 3 variant (H3.3) of *P. berghei*

In humans, there are a number of H3 variants outside of the 'canonical' H3.1 and H3.2 histones. There are two other 'main' H3 histones encoded for by the human genome: the replacement variant H3.3, and the centromere-specific H3, CENP-A (Shi, Wen and Shi, 2016). In humans, variant H3.3 can be incorporated into chromatin during replication at the cells synthesis phase (S-phase) or in a replication independent manner in non-dividing cells (Shi, Wen and Shi, 2016). The *P. berghei* ANKA genome also encodes for a H3.3 histone variant (PBANKA_1117100) that is identical to H3.3 sequences of 5 human-infective *Plasmodium* species, including both strains of *P. knowlesi* **(Figure S4)**.

When compared to mammalian H3.3 sequences (which are all identical to each other), *P. berghei* ANKA H3.3 differs at only 16 of 136 amino acids (89% sequence identity; blastp results not shown) (**Figure S4).** Most noticeable among these changes is the substitution of an arginine (R) for a lysine (K) at position 53, and a 5-residue substituted region in the N-terminal H3.3 tail from positions 31-25, though amino acid changes are often between residues with similar physiochemical properties (**Figure S4**).

```
CLUSTAL O(1.2.4) multiple sequence alignment


                                                                        ★    ★    ★   ★    ★   ★        ★★               ★  ★   
P_berghei_ANKA_(PBANKA_111710)                                      MARTKQTARKSTGGKAPRKQLASKAARKSAPVSTGIKKPHRYRPGTVALREIRKFQKSTD
P_falciparum_3D7_(PF3D7_0617900)                                    MARTKQTARKSTGGKAPRKQLASKAARKSAPVSTGIKKPHRYRPGTVALREIRKFQKSTD
P_vivax_Sal-1_(PVX_114020)                                          MARTKQTARKSTGGKAPRKQLASKAARKSAPVSTGIKKPHRYRPGTVALREIRKFQKSTD
P_knowlesi_strainH_(PKNH_1132500)                                   MARTKQTARKSTGGKAPRKQLASKAARKSAPVSTGIKKPHRYRPGTVALREIRKFQKSTD
P_knowlesi_strain_Malayan_Strain_PK1A_(PKNOH_S130199000)            MARTKQTARKSTGGKAPRKQLASKAARKSAPVSTGIKKPHRYRPGTVALREIRKFQKSTD
P_malariae_UG01_(PmUG01_11045700)                                   MARTKQTARKSTGGKAPRKQLASKAARKSAPVSTGIKKPHRYRPGTVALREIRKFQKSTD
P_ovale_curtisi_GH01_(PocGH01_11039400)                             MARTKQTARKSTGGKAPRKQLASKAARKSAPVSTGIKKPHRYRPGTVALREIRKFQKSTD
Mus_musculus_histone3.3_(P84244)                                    MARTKQTARKSTGGKAPRKQLATKAARKSAPSTGGVKKPHRYRPGTVALREIRRYQKSTE
Rattus_norvegicus_histone3.3_(NP_446437.1)                          MARTKQTARKSTGGKAPRKQLATKAARKSAPSTGGVKKPHRYRPGTVALREIRRYQKSTE
Homo_sapiens_(H3F3A)                                                MARTKQTARKSTGGKAPRKQLATKAARKSAPSTGGVKKPHRYRPGTVALREIRRYQKSTE
                                                                    **********************:******** : *:*****************::****:

                                                                        ★              ★                                   ★    
P_berghei_ANKA_(PBANKA_111710)                                      LLIRKLPFQRLVREIAQEYKTDLRFQSQAVLALQEAAEAYLVGLFEDTNLCAIHAKRVTI
P_falciparum_3D7_(PF3D7_0617900)                                    LLIRKLPFQRLVREIAQEYKTDLRFQSQAVLALQEAAEAYLVGLFEDTNLCAIHAKRVTI
P_vivax_Sal-1_(PVX_114020)                                          LLIRKLPFQRLVREIAQEYKTDLRFQSQAVLALQEAAEAYLVGLFEDTNLCAIHAKRVTI
P_knowlesi_strainH_(PKNH_1132500)                                   LLIRKLPFQRLVREIAQEYKTDLRFQSQAVLALQEAAEAYLVGLFEDTNLCAIHAKRVTI
P_knowlesi_strain_Malayan_Strain_PK1A_(PKNOH_S130199000)            LLIRKLPFQRLVREIAQEYKTDLRFQSQAVLALQEAAEAYLVGLFEDTNLCAIHAKRVTI
P_malariae_UG01_(PmUG01_11045700)                                   LLIRKLPFQRLVREIAQEYKTDLRFQSQAVLALQEAAEAYLVGLFEDTNLCAIHAKRVTI
P_ovale_curtisi_GH01_(PocGH01_11039400)                             LLIRKLPFQRLVREIAQEYKTDLRFQSQAVLALQEAAEAYLVGLFEDTNLCAIHAKRVTI
Mus_musculus_histone3.3_(P84244)                                    LLIRKLPFQRLVREIAQDFKTDLRFQSAAIGALQEASEAYLVGLFEDTNLCAIHAKRVTI
Rattus_norvegicus_histone3.3_(NP_446437.1)                          LLIRKLPFQRLVREIAQDFKTDLRFQSAAIGALQEASEAYLVGLFEDTNLCAIHAKRVTI
Homo_sapiens_(H3F3A)                                                LLIRKLPFQRLVREIAQDFKTDLRFQSAAIGALQEASEAYLVGLFEDTNLCAIHAKRVTI
                                                                    *****************::******** *: *****:***********************

                                                                      ★
P_berghei_ANKA_(PBANKA_111710)                                      MPKDIQLARRIRGERS
P_falciparum_3D7_(PF3D7_0617900)                                    MPKDIQLARRIRGERS
P_vivax_Sal-1_(PVX_114020)                                          MPKDIQLARRIRGERS
P_knowlesi_strainH_(PKNH_1132500)                                   MPKDIQLARRIRGERS
P_knowlesi_strain_Malayan_Strain_PK1A_(PKNOH_S130199000)            MPKDIQLARRIRGERS
P_malariae_UG01_(PmUG01_11045700)                                   MPKDIQLARRIRGERS
P_ovale_curtisi_GH01_(PocGH01_11039400)                             MPKDIQLARRIRGERS
Mus_musculus_histone3.3_(P84244)                                    MPKDIQLARRIRGERA
Rattus_norvegicus_histone3.3_(NP_446437.1)                          MPKDIQLARRIRGERA
Homo_sapiens_(H3F3A)                                                MPKDIQLARRIRGERA
                                                                    ***************:
```

Figure S4: Clustal alignment of *Plasmodium spp*. variant histone 3.3 (H3.3). This image shows a Clustal alignment of variant histone 3.3 (H3.3) amino acid sequences from *P. berghei* ANKA, *P. vivax* isolate Salvador 1 (Sal-1), *P. malariae* Uganda 01 (UG01) isolate, *P. falciparum* strain 3D7, *P. ovale curtisi* Ghana 01 isolate (Poc GH01), *P. knowlesi* macaque-adapted experimental strain H, *P. knowlesi* Malayan strain Pk1A, and mammalian species, *M. musculus, R. norvegicus,* and *H. sapiens sapiens*. The H3.3 sequences are 100% identical among *Plasmodium* species, and 100% between mammals. The *P. berghei* ANKA H3.3 differs from the mammalian H3.3 at 16 of 136 aa (maintaining 89% sequence identity).

In this image, lysines are again indicated by a star (★) above the amino acid letter (K). In Clustal, an asterisk (*) below an aligned amino acid indicates that the amino acid is fully conserved. A colon (:) underneath an aligned amino acid indicates conservation between residues with strongly similar properties (scoring an equivalent of >0.5 the Gonnet PAM 250 matrix (Pearson, 2013)). A full stop/period (.) below an aligned amino acid indicates conservation of residues with weakly similar properties (roughly equivalent to a score of >0 but <0.5 on the Gonnet PAM 250 matrix (Pearson, 2013)). No symbol beneath an aligned amino acid signifies that there is no conservation of the amino acid or exchange for an amino acid with similar properties.

S1.4 The canonical histone 2A (H2A) of *P. berghei*

Among eukaryotic core histones, it is the H2A histone that exhibits the highest sequence divergence, with variants differing mostly at the C-terminus, including at

the functionally important C-terminal docking domain (Bönisch and Hake, 2012). In *P. berghei* ANKA, the genome contains coding sequences for one core H2A histone (PBANKA_111700) and one H2A variant (H2A.Z) (PBANKA_1217600). Among *Plasmodium spp.* canonical H2A proteins, *P. berghei* ANKA H2A shares 100% sequence identity with canonical H2A sequences of *P. vivax* Sal-1, *P. ovale curtisi* GH01, and both *P. knowlesi* strains (strain H and Malayan strain Pk1A) (**Figure S5**). With regard to *P. falciparum* 3D7, the *P. berghei* ANKA H2A shares 98% sequence identity at amino acid level (blastp results not shown), with *P. falciparum* 3D7 substituting a serine (S) in place of a valine (V) at position 12, and 2 amino acid changes and the loss of a threonine residue at its C-terminus (**Figure S5**). In fact, the canonical H2A of *P. falciparum* 3D7 is the only H2A that is composed of 132 aa as opposed to 133 aa in all other *Plasmodium spp.*

Comparing *P. berghei* ANKA with *P. berghei malariae* UG01 however, reveals 98% amino acid sequence identity once more, with only 2 amino acid substitutions at the C-terminal tail of H2A (blastp results not shown). Surprisingly, these substitutions are not identical to those seen in *P. falciparum* 3D7, and the substitution of a valine (V) in *P. malariae* to a serine (S) in *P. falciparum* is present, as it is when comparing *P. falciparum* to the other *Plasmodium spp.* H2A sequences (**Figure S5**). Overall, *P. malariae* UG01 shares 97% sequence identity with *P. falciparum* 3D7 (blastp results not shown).

When comparing the *P. berghei* ANKA canonical H2A to the amino acid sequences of mammalian canonical H2A, *P. berghei* H2A shares only 73% sequence identity with the human H2A type 1 protein sequence (encoded for by gene P0C0S8.2) and 73% sequence identity with the H2A type 1 sequences of *M. musculus* and *R. norvegicus* which are identical (blastp results not shown). Though canonical H2A subtypes in mammals are variable (Bönisch and Hake, 2012), there are noticeable differences to the N- and C- termini of the *Plasmodium spp.* H2A protein sequences (**Figure S5**). The lengthening of the *Plasmodium spp.* C-terminus by 3 amino acids, with a loss of lysine (K) residues at positions 125, 127 and 129 are particularly striking (**Figure S5**). In all eukaryotes, including *Plasmodium spp.*, the C-terminus of H2A is located at the DNA entry/exit site of the nucleosome, making variations to this site a powerful

indicator of nucleosome stability and dynamics. This DNA entry/exit site is amenable to binding of DNA, binding to the H1 linker histone in higher mammals, and to binding by other interacting factors (Bönisch and Hake, 2012).

At the N-terminus of canonical H2A, *Plasmodium spp*. H2A proteins have evolved to include additional lysine residues at positions 3, 10 and 20, with additional lysines again added at positions 35, 38 and 41. These latter changes are made at the exact point of the histone H2A loop 1 (positions 38-41), which interacts with the H4 loop 2 to form a DNA-binding domain. Changes to the structure of loop 1 are linked to changes in centromeric targeting (Luger *et al.*, 1997; Vermaak, Hayden and Henikoff, 2002; Bönisch and Hake, 2012). In *Plasmodium spp.*, changes to the loop 1 region of H2A may have important implications for DNA-binding capabilities of the *Plasmodium* nucleosome.

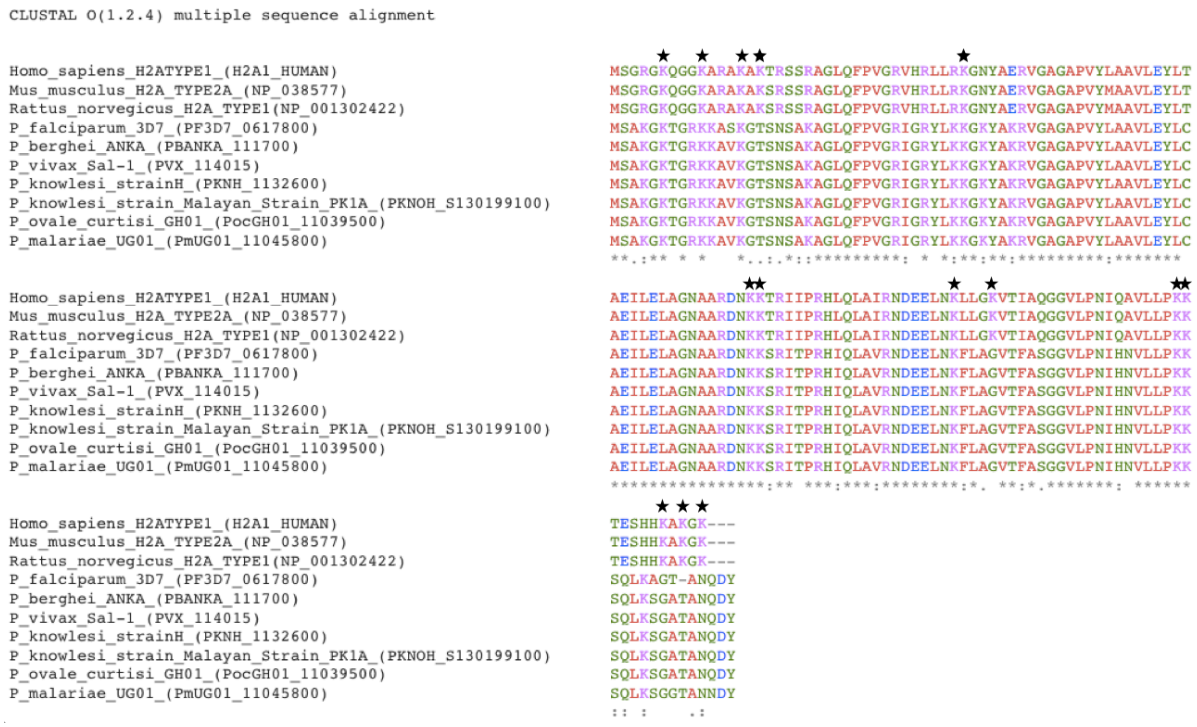

Figure S5: Clustal alignment of *Plasmodium spp*. canonical histone 2A (H2A). This image shows a Clustal alignment of canonical histone 2A (H2A) amino acid sequences from *P. berghei* ANKA, *P. vivax* isolate Salvador 1 (Sal-1), *P. malariae* Uganda 01 (UG01) isolate, *P. falciparum* strain 3D7, *P. ovale curtisi* Ghana 01 isolate (Poc GH01), *P. knowlesi* macaque-adapted experimental strain H, *P. knowlesi* Malayan strain Pk1A, and mammalian species, *M. musculus, R. norvegicus,* and *H. sapiens sapiens*. The canonical H2A sequences of *P. berghei* ANKA, *P. vivax* Sal-1, *P. ovale curtisi*, and both *P. knowlesi* strains are 100% identical. *P. falciparum* and *P. malariae* share 98% sequence identity with *P. berghei*

ANKA but differ in 3 and 2 amino acids respectively, with two amino acid substitutions each at the histone C-terminus. The *P. berghei* ANKA H2A sequence, and those of the other *Plasmodium spp.* differ considerably from the mammalian sequences, which is easily determined from the Clustal alignment above. Most noticeable is the loss of lysine residues at the C-terminal H2A end, with an extension of 3 amino acids also. The addition of further lysine residues at the N-terminus, and particularly at the Loop 1 region that is heavily involved in DNA interactions, suggests differing histone dynamics between *Plasmodium* parasites and higher order mammals.

In this image, lysines are indicated by a star (★) above the amino acid letter (K). In Clustal, an asterisk (*) below an aligned amino acid indicates that the amino acid is fully conserved. A colon (:) underneath an aligned amino acid indicates conservation between residues with strongly similar properties (scoring an equivalent of >0.5 the Gonnet PAM 250 matrix (Pearson, 2013)). A full stop/period (.) below an aligned amino acid indicates conservation of residues with weakly similar properties (roughly equivalent to a score of >0 but <0.5 on the Gonnet PAM 250 matrix (Pearson, 2013)). No symbol beneath an aligned amino acid signifies that there is no conservation of the amino acid or exchange for an amino acid with similar properties.

S1.5 The variant histone 2A (H2A.Z) of *P. berghei*

In eukaryotes, several histone 2A variants have been described, with some being vertebrate-specific, and others, such as H2A.Z and H2A.X, being conserved among many eukaryotic lineages (Malik and Henikoff, 2003). The variant H2A.X is conserved among many protists, including Giardia, and phosphorylation of this histone variant at the C-terminus has been described as a sensitive marker for DNA damage and the subsequent repair of a DNA lesion (Redon *et al.*, 2002; Sharma, Singh and Almasan, 2012). The other highly conserved H2A variant is H2A.Z, which can make up as much as ~10% of the H2A complement of an organism, and has been implicated in transcriptional activation and nucleosome stability (Redon *et al.*, 2002). In *Tetrahymena thermophila*, substitution of six N-terminal lysines to arginines proved lethal to the organism, with studies suggesting that acetylation of N-terminal lysines is responsible for modulation of an essential “charge patch” in *Tetrahymena* H2A.Z, with this “charge patch” being instrumental in the formation of histone-DNA and histone-protein interactions (Ren and Gorovsky, 2001; Redon *et al.*, 2002).

In *Plasmodium spp.,* only one H2A variant is encoded for in the genome, the highly conserved H2A variant, H2A.Z. In the mammals used for comparative analysis in this alignment, the H2A.Z amino acid sequences were 100% identical, and all were 128

aa in length (**Figure S6**; blastp results not shown). In contrast, all but one of the *Plasmodium spp*. H2A.Z sequences were 158 aa in length, with the outlier (*P. ovale curtisi* GH01) most probably diverging as a result of sequence error (**Figure S6**). The protein sequences for *P. vivax* Sal-1, *P. malariae* UG01, and both *P. knowlesi* strains were 100% identical. *P. berghei* ANKA shares 98% sequence identity with these human-infective *Plasmodium* species, differing at only 3 amino acid positions (blastp results not shown). With regard to the H2A.Z of *P. falciparum* 3D7, this parasite shares 96% sequence identity with *P. berghei* ANKA, and 97% sequence identity with other human-infective *Plasmodium spp*. (blastp results not shown). The amino acid substitutions between *Plasmodium* species were confined to position 6 in the N-terminus and positions 147 to 152 in the C-terminus (**Figure S6).**

Of course, the most compelling differences when observing an alignment of histone H2A.Z amino acid sequences between mammals and *Plasmodium spp*. are the striking extensions of both the H2A.Z N- and C- termini, with largely conserved sections of the core H2A.Z protein (**Figure S6**). At the amino terminus, the *Plasmodium spp*. H2A.Z sequence extends 23 aa upstream of the mammalian equivalent, with additional lysine residues at positions 5, 10, 14, 18 and 24 and maintaining the conserved H2A.Z K27. At the C-terminus, *Plasmodium spp*. H2A.Z extends 7 aa beyond its mammalian equivalent, with a lysine rich tail (lysines at positions 152, 153, 155 and 156) (when counting these lysines, the initial methionine of the amino acid sequence was not counted or counted as Met/M 0) (**Figure S6**). The presence of additional N-terminal lysines creates further positions at which acetylation of H2A.Z can occur, eliminating a positive charge at the N-terminus and allowing active transcription (Ren and Gorovsky, 2001; Redon *et al.*, 2002).

In yeast, the H2A.Z C-terminus, more specifically, the final 20 aa of the H2A.Z C-terminus, are crucial for incorporation of this histone variant to nucleosomes, and the ability of this histone to elicit its function as an antagonist of telomeric silencing (Meneghini, Wu and Madhani, 2003; A. Y. Wang *et al.*, 2011). In yeast, H2A.Z variants cluster near telomeres and antagonise heterochromatin spread by SIR2 enzymes (Meneghini, Wu and Madhani, 2003). Recruitment of H2A.Z during DNA strand break repair is also mediated by SUMOylation (incorporation of small ubiquitin-like

modifiers) at lysines 125 and 132 of the yeast H2A.Z sequence (Kalocsay, Hiller and Jentsch, 2009). In mammals, the K132 residue is lost but the K125 equivalent residue is present at position 120 of the H2A.Z amino acid sequence. In *Plasmodium spp*. the equivalent lysine is conserved at position 143 (**Figure S6)**. The addition of a lysine-rich C-terminal tail to the *Plasmodium spp*. H2A.Z opens up many possibilities for post-translational modifications that could alter chromatin-binding, telomeric de-silencing, and SUMOylation-based DNA repair mechanisms.

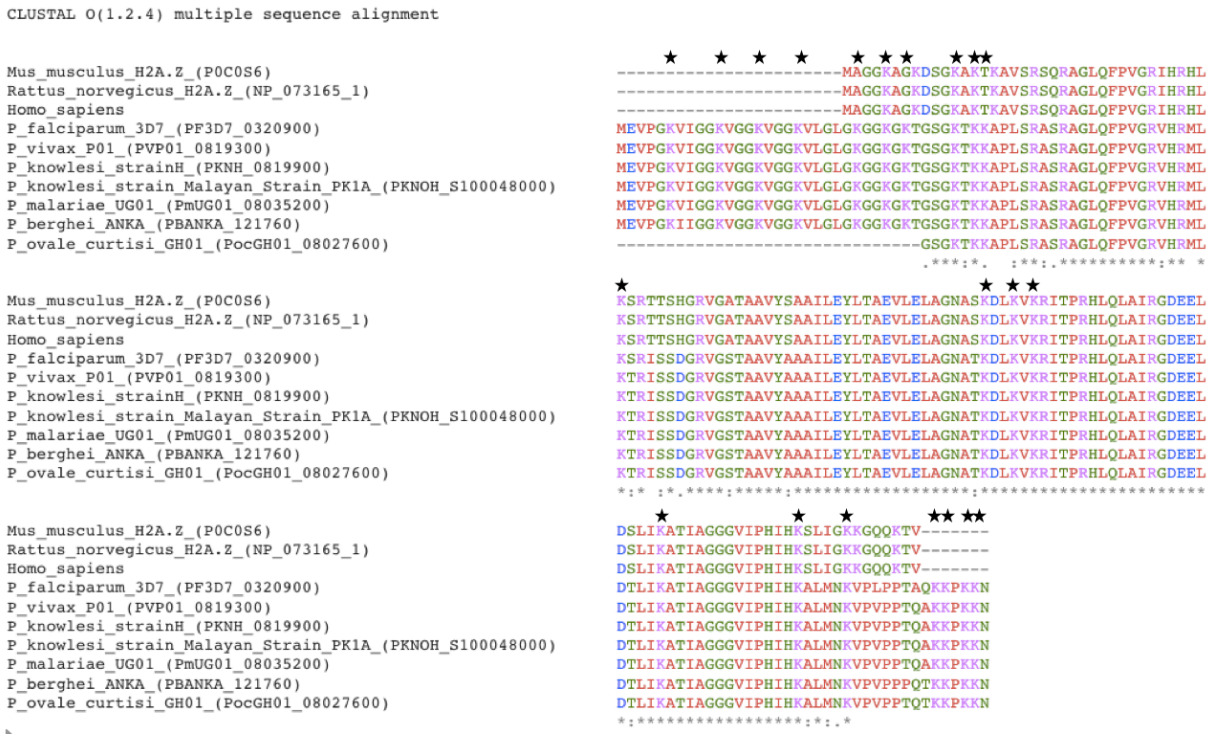

Figure S6: Clustal alignment of *Plasmodium spp*. variant 2A (H2A.Z). This image shows a Clustal alignment of variant histone 2A (H2A.Z) amino acid sequences from *P. berghei* ANKA, *P. vivax* isolate Salvador 1 (Sal-1), *P. malariae* Uganda 01 (UG01) isolate, *P. falciparum* strain 3D7, *P. ovale curtisi* Ghana 01 isolate (Poc GH01), *P. knowlesi* macaque-adapted experimental strain H, *P. knowlesi* Malayan strain Pk1A, and mammalian species, *M. musculus, R. norvegicus,* and *H. sapiens sapiens*. The H2A.Z sequences of *P. vivax* Sal-1, *P. malariae* UG01, and both *P. knowlesi* strains are 100% identical. *P. falciparum* and *P. berghei* ANKA share 97% and 96% sequence identity with these other *Plasmodium spp*. respectively, but the H2A.Z of *P. ovale curtisi* GH01 isolate assembly differs considerably, most likely owing to issues during genome assembly.

The *Plasmodium* H2A.Z sequences differ considerably from those of mammals at their extanded N- and C- termini. Ignoring the *P. ovale curtisi* GH01 assembly, all other *Plasmodium spp*. H2A.Z sequences include an additional 23 aa at their N-termini, and 7 extra amino acids at their C-terminal tails, many of these additions being lysine (K) residues that may be subject to post-translational

modification. In the above image, lysines are indicated by a star (★) above the amino acid letter (K), with all *Plasmodium* lysines indicated. The final shared lysine between mammalian and *Plasmodium* sequences is located at position 143 (K143), the equivalent of the yeast (*S. cerevisiae*) K125, which is SUMOylated in the event of DNA strand break repair.
In Clustal, an asterisk (*) below an aligned amino acid indicates that the amino acid is fully conserved. A colon (:) underneath an aligned amino acid indicates conservation between residues with strongly similar properties (scoring an equivalent of >0.5 the Gonnet PAM 250 matrix (Pearson, 2013)). A full stop/period (.) below an aligned amino acid indicates conservation of residues with weakly similar properties (roughly equivalent to a score of >0 but <0.5 on the Gonnet PAM 250 matrix (Pearson, 2013)). No symbol beneath an aligned amino acid signifies that there is no conservation of the amino acid or exchange for an amino acid with similar properties.

S1.6 The canonical histone 2B (H2B) of *P. berghei*

Unlike its dimerising partner (H2A), H2B in eukaryotes has very few variants (Malik and Henikoff, 2003). In humans, H2B has 16 isoforms: 13 of which are expressed in somatic cells and 3 of which are testis-specific (Molden *et al.*, 2015). In *Plasmodium spp.*, two H2B proteins are encoded for: canonical H2B and H2B.Z. In mammals, the *H. sapiens sapiens* H2B sequence shares 94% sequence identity with that of *M. musculus*, and 93% sequence identity with that of *R. norvegicus*, with all sequences being 127 aa in length (blastp results not shown). In comparison, all *Plasmodium spp.* H2B amino acid sequences are either 117 aa or 118 aa in length, all differing from the mammalian sequence at their amino termini (**Figure S7**).

Though the majority of the amino acid sequence of H2B is identical between *Plasmodium* species, only the H2B sequences of both *P. knowlesi* strains are 100% identical. These sequences, along with that of *P. falciparum* 3D7, are 117 aa in length and differ from the other *Plasmodium spp.* in that the A/T residue at position 15 has been lost (**Figure S7**). One notable difference between *Plasmodium* species however is at position 78, a position that contains a lysine in all mammalian H2B sequences, but which is swapped for an arginine in four of the seven *Plasmodium spp.* sequences (**Figure S7**). As in the mammalian H2B sequences, *P. berghei* ANKA, and both *P. knowlesi* strains maintain a K78 residue. However, in *P. falciparum* 3D7, *P. ovale curtisi* GH01, *P. malariae* UG01, and *P. vivax* Sal-1, this position is occupied

by R78. It is unknown whether this amino acid substitution may confer any functional differences to the H2B proteins of these particular *Plasmodium* isolates.

As can be discerned from **Figure S7**, there are few changes to the C-terminus of canonical H2B in *Plasmodium spp.* and this is most likely due to the presence of a C-terminal α-helix (αC) in H2B that is essential for its interaction with nucleosomal DNA. The final conserved lysine residue between mammals and *Plasmodium spp.* is at position 113 of the *Plasmodium* H2B sequences, a lysine that is mono-ubiquitinated at the C-terminal tail of H2B, and is responsible for modifications on H3 and H4 proteins (Malik and Henikoff, 2003). Inversely, the N-terminal tails of *Plasmodium spp.* H2B proteins can be distinguished from their mammalian equivalents by their loss of 9 amino acids, coupled with the loss of lysines at positions 6, 21, 24, and 25. These amino acid substitutions have the ability to make considerable changes to the overall structure of the H2B protein at its first α-helix (α1) (Malik and Henikoff, 2003).

Furthermore, the highly basic amino acid domain from positions 30-37 in the mammalian H2B, known as the histone H2B repression (HBR) domain, are not only retained in *Plasmodium spp.* (corresponding to positions 21-28), but are flanked by additional lysine residues from positions 18-20, indicating further possible mechanisms by which nucleosome assembly can be regulated by post-translational means in the malaria parasite (Mao *et al.*, 2016).

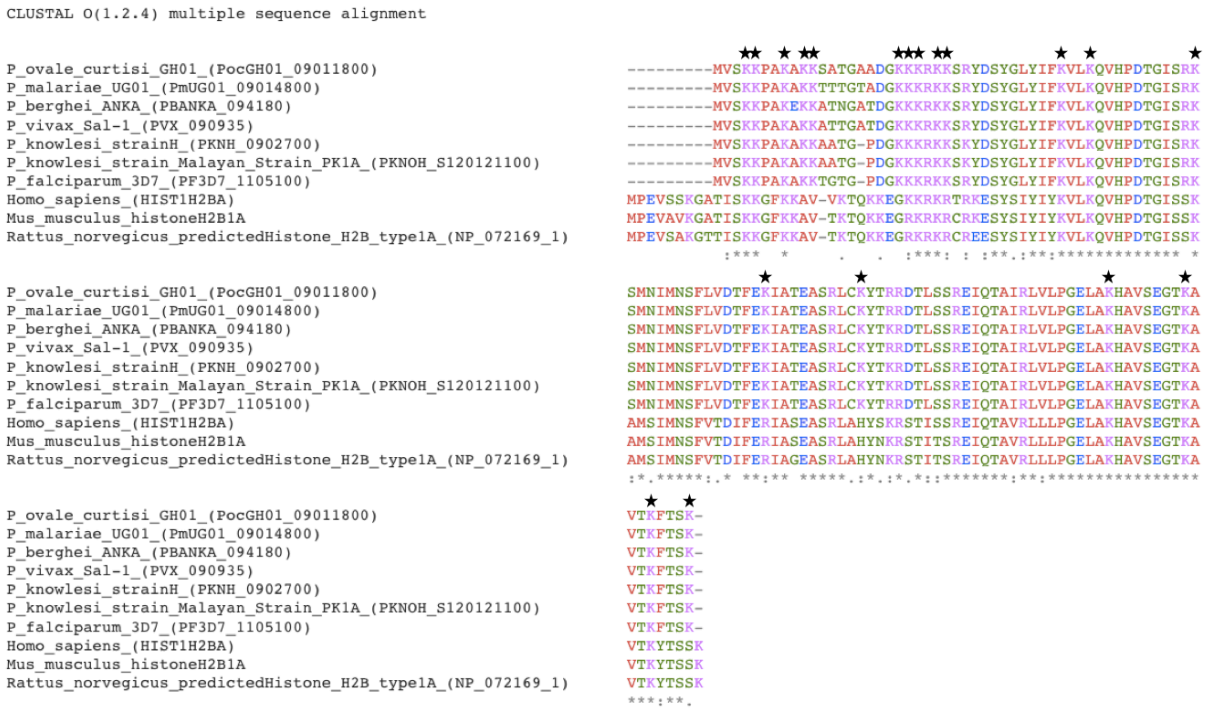

Figure S7: Clustal alignment of *Plasmodium spp*. canonical histone 2B (H2B). The image above shows a Clustal alignment of canonical histone 2B (H2B) amino acid sequences from *P. berghei* ANKA, *P. vivax* isolate Salvador 1 (Sal-1), *P. malariae* Uganda 01 (UG01) isolate, *P. falciparum* strain 3D7, *P. ovale curtisi* Ghana 01 isolate (Poc GH01), *P. knowlesi* macaque-adapted experimental strain H, *P. knowlesi* Malayan strain Pk1A, and mammalian species, *M. musculus, R. norvegicus,* and *H. sapiens sapiens*. The H2B sequences of all *Plasmodium spp.* differ slightly from one another, with the exception of both *P. knowlesi* strains. When comparing *Plasmodium* H2B to mammalian H2B, it is clear from a Clustal alignment that the amino termini of *Plasmodium spp.* H2B histones differ considerably from those of mammals. Though certain lysine residues are conserved, more have been added upstream of the histone H2B repression (HBR) domain (positions 21-28 in *Plasmodium spp.*) suggesting alterations at the secondary and tertiary structural level of H2B in *Plasmodium spp.* These changes may manifest functionally at different stages of the parasite life cycle. In the above image, lysines are indicated by a star (★) above the amino acid letter (K), with all *Plasmodium* lysines indicates.

In Clustal, an asterisk (*) below an aligned amino acid indicates that the amino acid is fully conserved. A colon (:) underneath an aligned amino acid indicates conservation between residues with strongly similar properties (scoring an equivalent of >0.5 the Gonnet PAM 250 matrix (Pearson, 2013)). A full stop/period (.) below an aligned amino acid indicates conservation of residues with weakly similar properties (roughly equivalent to a score of >0 but <0.5 on the Gonnet PAM 250 matrix (Pearson, 2013)). No symbol beneath an aligned amino acid signifies that there is no conservation of the amino acid or exchange for an amino acid with similar properties.

S1.7 The variant histone 2B (H2B.Z) of *P. berghei*

In *P. berghei*, there is only one variant histone H2B, termed H2B.Z, that most closely resembles the human H2B variant 1-L (63% sequence identity), the mouse H2B variant 1-B (63% sequence identity), and the rat H2B variant 1-B (63% sequence identity; blastp results not shown). Unlike the limited amount of information so far gleaned about the interactions and functions of other canonical and variant histone in *Plasmodium spp.*, the role of H2B.Z has been determined, at least in part, in *P. falciparum*. Using *P. falciparum* strain 3D7, it was established that H2A.Z/H2B.Z double-variant nucleosomes preferentially localise to euchromatic, AT-rich, intergenic regions, and demarcate promoters and putative epigenetic regulatory regions of the genome (Hoeijmakers *et al.*, 2013). In a second study, and using the same parasite, it was also determined that the H2A.Z/H2B.Z double-variant nucleosome was enriched at the promoter of the single active *var* gene, and so was implicated in control of monoallelic *var* gene expression and *P. falciparum* virulence (Petter *et al.*, 2013).

Though the role of H2A.Z/H2B.Z double-variant nucleosomes in the active transcription of a single *P. falciparum var* gene, and in marking promoters in euchromatin, are known at present (Hoeijmakers *et al.*, 2013; Petter *et al.*, 2013), it remains to be seen whether post-translational modifications of the H2B.Z variant histone can also play a role in modulating H2A.Z/H2B.Z-promoter occupancy, and to what extent such modifications can influence transitions from one parasite life cycle stage to another. Could modification of an H2B.Z residue affect H2A.Z/H2B.Z demarcation, and thus transcriptional activation, of an AP2 transcriptional regulator, for example?

When comparing the *Plasmodium spp.* H2B.Z amino acid sequences to those of the most similar mammalian H2B variants in human, rat and mouse, it can be seen that, once more (as with canonical H2B), the *Plasmodium spp.* H2B.Z differs most significantly at the amino terminus. In *Plasmodium* H2B.Z sequences, shortening of the N-terminal tails may have consequences for the α1 and α2 helices of the histone secondary structure (Malik and Henikoff, 2003). The H2B.Z C-terminus in *Plasmodium spp.* again remains the most unaltered portion of the histone variant

when compared with its mammalian counterpart, with retention of K116 (the amino acid position in *Plasmodium spp.*), and its flanking tyrosine (Y) and threonine (T) residues, possibly maintaining key roles in *trans*-histone H3-H4 methylation (Chandrasekharan *et al.*, 2010). Maintenance of threonine 115 (T115) in *Plasmodium spp.* sequences (homologous to the yeast T122) reinforces the idea that this region of H2B.Z is involved in conserved mechanisms of chromatin compaction and that modifications at these sites may have important consequences on histone-histone and histone-DNA binding (C. Y. Wang *et al.*, 2011).

When examining *Plasmodium spp.* H2B.Z sequences alone, all H2B.Z histones are 123 aa in length, with those of *P. berghei* ANKA, *P. vivax* Sal-1, *P. ovale curtisi* GH01, and both *P. knowlesi* strains being 100% identical (**Figure S8**). Both *P. malariae* UG01 and *P. falciparum* 3D7 H2B.Z sequences differ at only one amino acid each. In histone H2B.Z of *P. malariae* UG01, a serine (S) at position 9 in other *Plasmodium* species is replaced by an alanine (A). In *P. falciparum* H2B.Z, a glycine (G) at position 121 (not counting the initial methionine residue) is replaced by an alanine (A). All other amino acid positions remain identical.

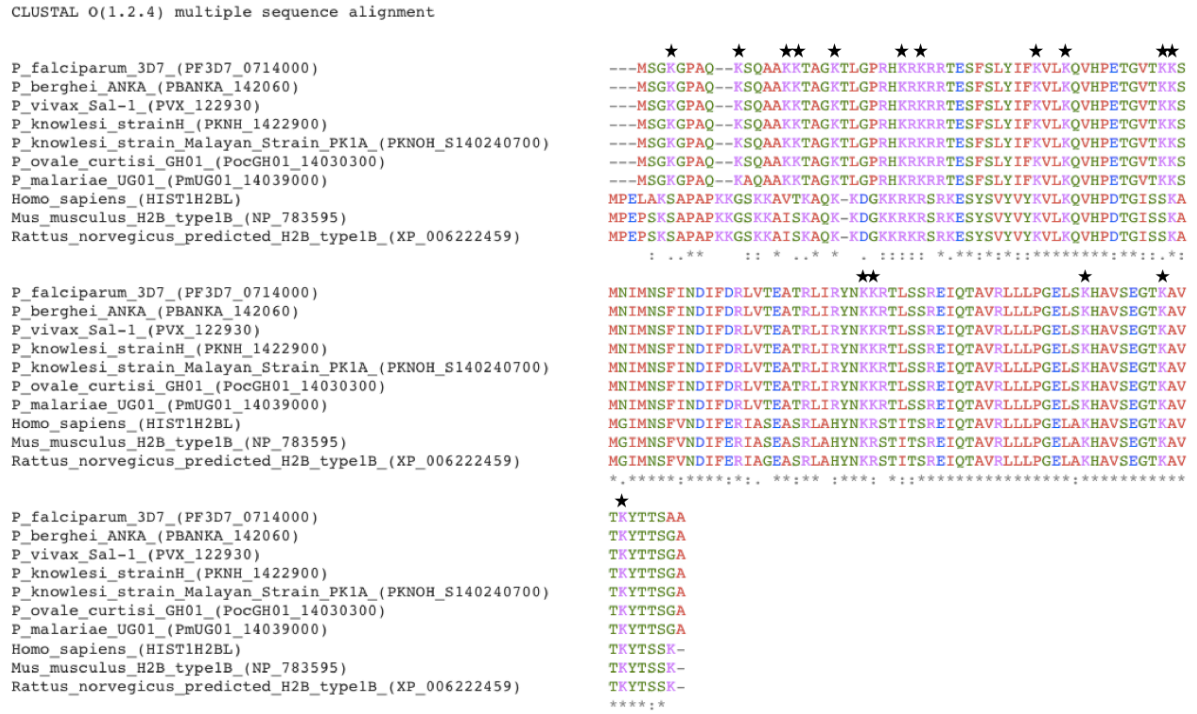

Figure S8: Clustal alignment of *Plasmodium spp.* variant histone 2B (H2B.Z). The image above shows a Clustal alignment of variant histone 2B (H2B.Z) amino acid sequences from *P. berghei* ANKA,

P. vivax isolate Salvador 1 (Sal-1), *P. malariae* Uganda 01 (UG01) isolate, *P. falciparum* strain 3D7, *P. ovale curtisi* Ghana 01 isolate (Poc GH01), *P. knowlesi* macaque-adapted experimental strain H, *P. knowlesi* Malayan strain Pk1A, and mammalian species, *M. musculus, R. norvegicus,* and *H. sapiens sapiens*. The H2B.Z amino acid sequences of *Plasmodium spp.* are remarkably similar. The H2B.Z sequences of *P. berghei* ANKA, *P. ovale curtisi* GH01, *P. vivax* Sal-1, and both *P. knowlesi* strains, are 100% identical. *P. falciparum* 3D7, and *P. malariae* UG01 H2B.Z sequences each differ at only one amino acid position each (mutations G121A and S9A respectively). Between *Plasmodium spp.* and the closest mammalian H2B variants, the C-termini of all sequences remain similar, but with alterations to the N-termini that may manifest in the secondary α1 and α2 helices structures of the H2B.Z protein. In the above image, all *Plasmodium spp.* lysines are indicated by a star (★).
In Clustal, an asterisk (*) below an aligned amino acid indicates that the amino acid is fully conserved. A colon (:) underneath an aligned amino acid indicates conservation between residues with strongly similar properties (scoring an equivalent of >0.5 the Gonnet PAM 250 matrix (Pearson, 2013)). A full stop/period (.) below an aligned amino acid indicates conservation of residues with weakly similar properties (roughly equivalent to a score of >0 but <0.5 on the Gonnet PAM 250 matrix (Pearson, 2013)). No symbol beneath an aligned amino acid signifies that there is no conservation of the amino acid or exchange for an amino acid with similar properties.

S1.8 The histone H3-like centromeric protein CSE4 (CenH3) of *P. berghei*

In eukaryotes, centromere-specific H3 variants (CenH3s) are specialised H3 variants for chromatin packaging during mitosis and are atypical, rapidly evolving H3 variant histones (Malik and Henikoff, 2003). In *P. falciparum* 3D7, the CenH3 variant histone occupies a 4-4.5 kb region of each of the 14 chromosomes and localises to a single nuclear location prior to mitosis and cytokinesis (Hoeijmakers *et al.*, 2012). Using *P. falciparum* strain FCK2 (a local strain to Karnataka, India), the ability of the *Pf*CenH3 to complement the loss of its homologue in yeast (Cse4p) demonstrated its ability to mark active centromeres for kinetochore assembly, and therefore to facilitate chromosome segregation (Verma and Surolia, 2013).

A comparison of the amino acid sequences of the CenH3 histones of human, rat, and mouse, and between *Plasmodium* species, highlights the rapid evolution of this H3 variant (**Figure S9**). Between *Plasmodium* species alone, only the *P. knowlesi* strains share an identical CenH3 protein, with this sequence sharing 87% sequence identity with *P. vivax* Sal-1, 74% sequence identity with both *P. malariae* UG01 and *P. falciparum* 3D7, 73% sequence identity with *P. ovale curtisi* GH01, and 68% sequence

identity with *P. berghei* ANKA (blastp results not shown). Among all CenH3 histones, including those of mammals, it is the essential C-terminal end that shows the highest conservation (**Figure S9**). In the *P. falciparum*/*S. cerevisiae* complementation study (Verma and Surolia, 2013), the carboxy terminal histone fold domain (HFD) that harbours a CENP-A targeting domain (CATD) (termed CENP-C in *P. falciparum*), was indispensable for centromeric-targeting and CenH3 function.

Between all mammal and *Plasmodium* species shown in **Figure S9**, it is the N-termini that have evolved most rapidly, in line with other eukaryotic lineages (Malik and Henikoff, 2003). In *Plasmodium* CenH3 sequences, a lysine pair (K4 and K5) is conserved among all species at the N-terminus, a site that is perhaps targetable for post-translational modification, though no such modifications have been identified to date (Trelle *et al.*, 2009; Coetzee *et al.*, 2017).

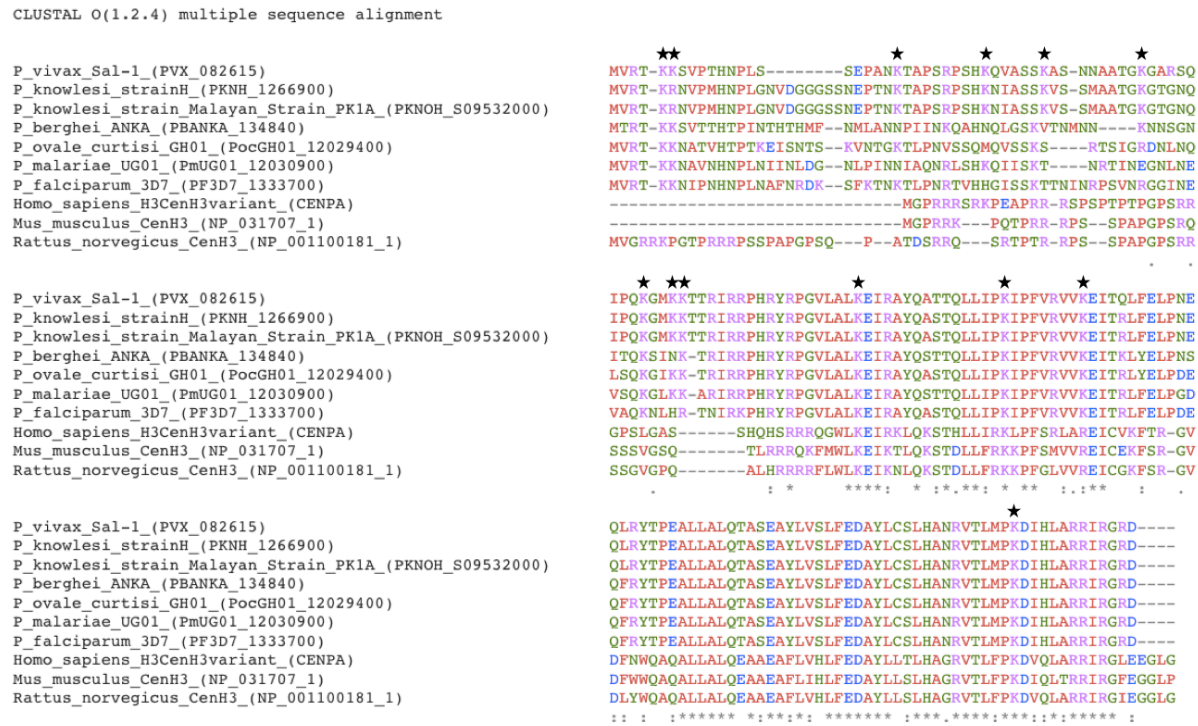

Figure S9: Clustal alignment of *Plasmodium spp*. variant histone H3-like CSE4 proteins and mammalian centromere-specific histone 3 (CenH3). This image shows a Clustal alignment of the variant centromere-specific H3 histones (CenH3s) of *M. musculus*, *R. norvegicus*, and *H. sapiens sapiens*, in comparison with the equivalent histone H3-like CSE4 protein sequences of *P. berghei* ANKA, *P. vivax* isolate Salvador 1 (Sal-1), *P. malariae* Uganda 01 (UG01) isolate, *P. falciparum* strain 3D7, *P. ovale curtisi* Ghana 01 isolate (Poc GH01), *P. knowlesi* macaque-adapted experimental strain

H, and *P. knowlesi* Malayan strain Pk1A. In all aligned sequences, the C-termini of CenH3 proteins show quite significant conservation, likely owing to the essentiality of the C-terminus of CenH3 for centromeric-targeting and correct chromosome segregation during mitosis. As the sequence reaches the amino terminus, the CenH3 protein shows signs of evolution, even between *Plasmodium spp.* Though an initial K4/K5 pair is conserved among *Plasmodium* sequences, CenH3 sequences differ considerably, often with deletions of a series of amino acids. In this image, all *Plasmodium spp.* lysines are indicated by a star (★) above the sequence.

In Clustal, an asterisk (*) below an aligned amino acid indicates that the amino acid is fully conserved. A colon (:) underneath an aligned amino acid indicates conservation between residues with strongly similar properties (scoring an equivalent of >0.5 the Gonnet PAM 250 matrix (Pearson, 2013)). A full stop/period (.) below an aligned amino acid indicates conservation of residues with weakly similar properties (roughly equivalent to a score of >0 but <0.5 on the Gonnet PAM 250 matrix (Pearson, 2013)). No symbol beneath an aligned amino acid signifies that there is no conservation of the amino acid or exchange for an amino acid with similar properties.

Supplemental Information S1 References

Altschul, S. F., Gish, W., Miller, W., Myers, E. W. and Lipman, D. J. (1990) 'Basic local alignment search tool', *Journal of Molecular Biology*, 215(3):403–410.

Artavanis-Tsakonas, K., Misaghi, S., Comeaux, C. A., Catic, A., Spooner, E., Duraisingh, M. T. and Ploegh, H. L. (2006) 'Identification by functional proteomics of a deubiquitinating/deNeddylating enzyme in *Plasmodium falciparum*', *Molecular Microbiology*, 61(5): 1187–1195.

Artavanis-Tsakonas, K., Weihofen, W. A., Antos, J. M., Coleman, B. I., Comeaux, C. A., Duraisingh, M. T., Gaudet, R. and Ploegh, H. L. (2010) 'Characterization and structural studies of the *Plasmodium falciparum* ubiquitin and Nedd8 hydrolase UCHL3', *Journal of Biological Chemistry*, 285(9): 6857–6866.

Bönisch, C. and Hake, S. B. (2012) 'Histone H2A variants in nucleosomes and chromatin: More or less stable?', *Nucleic Acids Research*, 40(21): 10719–10741.

Braks, J. A. M., Mair, G. R., Franke-Fayard, B., Janse, C. J. and Waters, A. P. (2008) 'A conserved U-rich RNA region implicated in regulation of translation in *Plasmodium* female gametocytes', *Nucleic Acids Research*, 36(4): 1176–1186.

Brancucci, N. M. B., Bertschi, N. L., Zhu, L., Niederwieser, I., Chin, W. H., Wampfler, R., Freymond, C., Rottmann, M., Felger, I., Bozdech, Z. and Voss, T. S. (2014) 'Heterochromatin protein 1 secures survival and transmission of malaria parasites', *Cell Host and Microbe*, 16(2): 165–176.

Carvalho, T. G. and Ménard, R. (2005) 'Manipulating the *Plasmodium* genome', *Current Issues in Molecular Biology*, pp. 39–56.

Chaal, B. K., Gupta, A. P., Wastuwidyaningtyas, B. D., Luah, Y.-H. and Bozdech, Z. (2010) 'Histone deacetylases play a major role in the transcriptional regulation of the *Plasmodium falciparum* life cycle.', *PLoS pathogens*, 6(1): e1000737. doi: 10.1371/journal.ppat.1000737.

Chandrasekharan, M. B., Huang, F., Chen, Y.-C. and Sun, Z.-W. (2010) 'Histone H2B C-Terminal Helix Mediates trans-Histone H3K4 Methylation Independent of H2B Ubiquitination', *Molecular and Cellular Biology*, 30(13): 3216–3232.

Chen, P. B., Ding, S., Zanghì, G., Soulard, V., Dimaggio, P. A., Fuchter, M. J., Mecheri, S., Mazier, D., Scherf, A. and Malmquist, N. A. (2016) '*Plasmodium falciparum* PfSET7: enzymatic characterization and cellular localization of a novel protein methyltransferase in sporozoite, liver and erythrocytic stage parasites', *Scientific reports*, 6: 21802. doi: 10.1038/srep21802.

Coetzee, N., Sidoli, S., van Biljon, R., Painter, H., Llinás, M., Garcia, B. A. and Birkholtz, L.-M. (2017) 'Quantitative chromatin proteomics reveals a dynamic histone post-translational modification landscape that defines asexual and sexual *Plasmodium falciparum* parasites.', *Scientific reports*, 7(1): 607. doi: 10.1038/s41598-017-00687-7.

Coleman, B. I., Skillman, K. M., Jiang, R. H. Y., Childs, L. M., Altenhofen, L. M., Ganter, M., Leung, Y., Goldowitz, I., Kafsack, B. F. C., Marti, M., Llinás, M., Buckee, C. O. and Duraisingh, M. T. (2014) 'A *Plasmodium falciparum* Histone Deacetylase regulates antigenic variation and gametocyte conversion', *Cell Host and Microbe*, 16(2): 177–186.

Cui, L., Fan, Q., Cui, L. and Miao, J. (2008) 'Histone lysine methyltransferases and demethylases in *Plasmodium falciparum*', *International Journal for Parasitology*, 38(10): 1083–1097.

Cui, L. and Miao, J. (2010) 'Chromatin-Mediated epigenetic regulation in the malaria parasite *Plasmodium falciparum*', *Eukaryotic Cell*, 1138–1149. doi: 10.1128/EC.00036-10.

Duffy, M. F., Selvarajah, S. A., Josling, G. A. and Petter, M. (2013) 'Epigenetic regulation of the P*lasmodium falciparum* genome'. doi: 10.1093/bfgp/elt047.

Fan, Q., An, L. and Cui, L. (2004a) 'PfADA2, a *Plasmodium falciparum* homologue of the transcriptional coactivator ADA2 and its in vivo association with the histone acetyltransferase PfGCN5', *Gene*, 336(2): 251–261.

Fan, Q., An, L. and Cui, L. (2004b) '*Plasmodium falciparum* histone acetyltransferase, a yeast GCN5 homologue involved in chromatin remodeling', *Eukaryotic Cell*, 3(2): 264–276.

Fréville, A., Landrieu, I., García-Gimeno, M. A., Vicogne, J., Montbarbon, M., Bertin, B., Verger, A., Kalamou, H., Sanz, P., Werkmeister, E., Pierrot, C. and

Khalife, J. (2012) '*Plasmodium falciparum* inhibitor-3 homolog increases protein phosphatase type 1 activity and is essential for parasitic survival', *Journal of Biological Chemistry*, 287(2): 1306–1321.

Gonnet, G., Cohen, M. and Benner, S. (1992) 'Exhaustive matching of the entire protein sequence database', *Science*, 256(5062): 1443–1445.

Hoeijmakers, W. A. M., Flueck, C., Françoijs, K. J., Smits, A. H., Wetzel, J., Volz, J. C., Cowman, A. F., Voss, T., Stunnenberg, H. G. and Bártfai, R. (2012) '*Plasmodium falciparum* centromeres display a unique epigenetic makeup and cluster prior to and during schizogony', *Cellular Microbiology*, 14(9):1391–1401.

Hoeijmakers, W. A. M., Salcedo-Amaya, A. M., Smits, A. H., Françoijs, K.-J. J., Treeck, M., Gilberger, T.-W. W., Stunnenberg, H. G. and Bártfai, R. (2013) 'H2A.Z/H2B.Z double-variant nucleosomes inhabit the AT-rich promoter regions of the *Plasmodium falciparum* genome.', *Molecular Microbiology*, 87(5): 1061–73.

Horrocks, P., Wong, E., Russell, K. and Emes, R. D. (2009) 'Control of gene expression in *Plasmodium falciparum* - Ten years on', *Molecular and Biochemical Parasitology*, pp. 9–25. doi: 10.1016/j.molbiopara.2008.11.010.

Janse, C. J., Boorsma, E. G., Ramesar, J., Van Der Meer, R., Zenobi, P., Casaglia, 0, Mons, B., Van Der Berct, F. M. and Vianen, V. (1989) '*Plasmodium berghei*: Gametocyte Production, DNA Content, and Chromosome-Size Polymorphisms during Asexual Multiplication in Vivo', *Experimental Parasitology*, 68: 274–282.

Janse, C. J., Ramesar, J. and Waters, A. P. (2006) 'High-efficiency transfection and drug selection of genetically transformed blood stages of the rodent malaria parasite *Plasmodium berghei*', *Nature Protocols*, 1(1): 346–356.

Jiang, L., Mu, J., Zhang, Q., Ni, T., Srinivasan, P., Rayavara, K., Yang, W., Turner, L., Lavstsen, T., Theander, T. G., Peng, W., Wei, G., Jing, Q., Wakabayashi, Y., Bansal, A., Luo, Y., Ribeiro, J. M. C., Scherf, A., Aravind, L., Zhu, J., Zhao, K. and Miller, L. H. (2013) 'PfSETvs methylation of histone H3K36 represses virulence genes in *Plasmodium falciparum*.', *Nature*, 499(7457):

223–7.

Joshi, M. B., Lin, D. T., Chiang, P. H., Goldman, N. D., Fujioka, H., Aikawa, M. and Syin, C. (1999) 'Molecular cloning and nuclear localization of a histone deacetylase homologue in *Plasmodium falciparum*', *Molecular and Biochemical Parasitology*, 99(1): 11–19.

Josling, G. A., Petter, M., Oehring, S. C., Gupta, A. P., Dietz, O., Wilson, D. W., Schubert, T., Längst, G., Gilson, P. R., Crabb, B. S., Moes, S., Jenoe, P., Lim, S. W., Brown, G. V., Bozdech, Z., Voss, T. S. and Duffy, M. F. (2015) 'A *Plasmodium Falciparum* Bromodomain Protein Regulates Invasion Gene Expression', *Cell Host and Microbe*, 17(6): 741–751.

Kalocsay, M., Hiller, N. J. and Jentsch, S. (2009) 'Chromosome-wide Rad51 Spreading and SUMO-H2A.Z-Dependent Chromosome Fixation in Response to a Persistent DNA Double-Strand Break', *Molecular Cell*, 33(3): 335–343.

Kanyal, A., Rawat, M., Gurung, P., Choubey, D., Anamika, K. and Karmodiya, K. (2018) 'Genome-wide survey and phylogenetic analysis of histone acetyltransferases and histone deacetylases of *Plasmodium falciparum*', *The FEBS Journal*. doi: 10.1111/febs.14376.

Kumar, A., Bhowmick, K., Vikramdeo, K. S., Mondal, N., Subbarao, N. and Dhar, S. K. (2017) 'Designing novel inhibitors against histone acetyltransferase (HAT: GCN5) of *Plasmodium falciparum*', *European Journal of Medicinal Chemistry*, 138: 26–37.

Lapp, S. A., Geraldo, J. A., Chien, J. T., Ay, F., Pakala, S. B., Batugedara, G., Humphrey, J., Debarry, J. D., Le Roch, K. G., Galinski, M. R. And Kissinger, J. C. (2017) 'PacBio assembly of a *Plasmodium knowlesi* genome sequence with Hi-C correction and manual annotation of the SICAvar gene family', *Parasitology*, pp. 1–14. doi: 10.1017/S0031182017001329.

Latreille, D., Bluy, L., Benkirane, M. and Kiernan, R. E. (2014) 'Identification of histone 3 variant 2 interacting factors', *Nucleic Acids Research*, 42(6): 3542–3550.

Lee, R. S., Waters, A. P. and Brewer, J. M. (2018) 'A cryptic cycle in haematopoietic niches promotes initiation of malaria transmission and evasion of

chemotherapy', *Nature Communications,* 9(1): 1689. doi: 10.1038/s41467-018-04108-9.

Luger, K., Mäder, A. W., Richmond, R. K., Sargent, D. F. and Richmond, T. J. (1997) 'Crystal structure of the nucleosome core particle at 2.8 Å resolution', *Nature*, 389(6648): 251–260.

Maehara, K., Harada, A., Sato, Y., Matsumoto, M., Nakayama, K. I., Kimura, H. and Ohkawa, Y. (2015) 'Tissue-specific expression of histone H3 variants diversified after species separation', *Epigenetics and Chromatin*, 8(1). doi: 10.1186/s13072-015-0027-3.

Malik, H. S. and Henikoff, S. (2003) 'Phylogenomics of the nucleosome', *Nature Structural & Molecular Biology*, 10(11): 882–891.

Mancio-Silva, L., Lopez-Rubio, J. J., Claes, A. and Scherf, A. (2013) 'Sir2a regulates rDNA transcription and multiplication rate in the human malaria parasite *Plasmodium falciparum*.', *Nature communications*, 4: 1530. doi: 10.1038/ncomms2539.

Manzoni, G., Briquet, S., Risco-Castillo, V., Gaultier, C., Topçu, S., Ivănescu, M. L., Franetich, J.-F., Hoareau-Coudert, B., Mazier, D. and Silvie, O. (2015) 'A rapid and robust selection procedure for generating drug-selectable marker-free recombinant malaria parasites', *Scientific Reports*, 4(1): 4760.

Mao, P., Kyriss, M. N. M., Hodges, A. J., Duan, M., Morris, R. T., Lavine, M. D., Topping, T. B., Gloss, L. M. and Wyrick, J. J. (2016) 'A basic domain in the histone H2B N-terminal tail is important for nucleosome assembly by FACT', *Nucleic Acids Research*, 44(19): 9142–9152.

Meneghini, M. D., Wu, M. and Madhani, H. D. (2003) 'Conserved histone variant H2A.Z protects euchromatin from the ectopic spread of silent heterochromatin', *Cell*, 112(5): 725–736.

Merrick, C. J., Dzikowski, R., Imamura, H., Chuang, J., Deitsch, K. and Duraisingh, M. T. (2010) 'The effect of *Plasmodium falciparum* Sir2a histone deacetylase on clonal and longitudinal variation in expression of the var family of virulence genes', *International Journal for Parasitology*, 40(1): 35–43.

Merrick, C. J., Huttenhower, C., Buckee, C., Amambua-Ngwa, A., Gomez-Escobar,

N., Walther, M., Conway, D. J. and Duraisingh, M. T. (2012) 'Epigenetic dysregulation of virulence gene expression in severe *Plasmodium falciparum* malaria.', *The Journal of infectious diseases*, 205(10): 1593–600.

Miao, J., Fan, Q., Cui, L., Li, X., Wang, H., Ning, G., Reese, J. C. and Cui, L. (2010) 'The MYST family histone acetyltransferase regulates gene expression and cell cycle in malaria parasite *Plasmodium falciparum*', *Molecular Microbiology*, 78(4): 883–902.

Molden, R. C., Bhanu, N. V, LeRoy, G., Arnaudo, A. M. and Garcia, B. A. (2015) 'Multi-faceted quantitative proteomics analysis of histone H2B isoforms and their modifications', *Epigenetics & Chromatin*, 8(1): 15. doi: 10.1186/s13072-015-0006-8.

Pearson, W. R. (2013) 'Selecting the Right Similarity-Scoring Matrix.', *Current protocols in bioinformatics*, 43: 3.5.1-9. doi: 10.1002/0471250953.bi0305s43.

Petter, M., Lee, C. C., Byrne, T. J., Boysen, K. E., Volz, J., Ralph, S. A., Cowman, A. F., Brown, G. V. and Duffy, M. F. (2011) 'Expression of *P. falciparum var* genes involves exchange of the histone variant H2A.Z at the promoter', *PLoS Pathogens*, 7(2). doi: 10.1371/journal.ppat.1001292.

Petter, M., Selvarajah, S. A., Lee, C. C., Chin, W. H., Gupta, A. P., Bozdech, Z., Brown, G. V. and Duffy, M. F. (2013) 'H2A.Z and H2B.Z double-variant nucleosomes define intergenic regions and dynamically occupy var gene promoters in the malaria parasite *Plasmodium falciparum*', *Molecular Microbiology*, 87(6): 1167–1182.

Pfander, C., Anar, B., Brochet, M., Rayner, J. C. and Billker, O. (2013) 'Recombination-mediated genetic engineering of *Plasmodium berghei* DNA', *Methods in Molecular Biology*, 923: 127–138.

Philip, N. and Waters, A. P. (2015) 'Conditional Degradation of *Plasmodium* Calcineurin Reveals Functions in Parasite Colonization of both Host and Vector.', *Cell host & microbe*, 18(1): 122–31.

Ponzi, M., Sidén-Kiamos, I., Bertuccini, L., Currà, C., Kroeze, H., Camarda, G., Pace, T., Franke-Fayard, B., Laurentino, E. C., Louis, C., Waters, A. P., Janse, C. J. and Alano, P. (2009) 'Egress of *Plasmodium berghei* gametes from

their host erythrocyte is mediated by the MDV-1/PEG3 protein', *Cellular Microbiology*, 11(8): 1272–1288.

Poran, A., Nötzel, C., Aly, O., Mencia-Trinchant, N., Harris, C. T., Guzman, M. L., Hassane, D. C., Elemento, O. and Kafsack, B. F. C. (2017) 'Single-cell RNA sequencing reveals a signature of sexual commitment in malaria parasites', *Nature*, 551(7678): 95. doi: 10.1038/nature24280.

Redon, C., Pilch, D., Rogakou, E., Sedelnikova, O., Newrock, K. and Bonner, W. (2002) 'Histone H2A variants H2AX and H2AZ', *Current Opinion in Genetics and Development*, pp. 162–169. doi: 10.1016/S0959-437X(02)00282-4.

Ren, Q. and Gorovsky, M. A. (2001) 'Histone H2A.Z acetylation modulates an essential charge patch', *Molecular Cell*, 7(6): 1329–1335.

Rono, M. K., Nyonda, M. A., Simam, J. J., Ngoi, J. M., Mok, S., Kortok, M. M., Abdullah, A. S., Elfaki, M. M., Waitumbi, J. N., El-Hassan, I. M., Marsh, K., Bozdech, Z. and Mackinnon, M. J. (2017) 'Adaptation of *Plasmodium falciparum* to its transmission environment', *Nature Ecology and Evolution*, pp. 1–11. doi: 10.1038/s41559-017-0419-9.

Schwach, F., Bushell, E., Gomes, A. R., Anar, B., Girling, G., Herd, C., Rayner, J. C. and Billker, O. (2015) '*Plasmo*GEM, a database supporting a community resource for large-scale experimental genetics in malaria parasites', *Nucleic Acids Research*, 43(D1): D1176–D1182. doi: 10.1093/nar/gku1143.

Sharma, A., Singh, K. and Almasan, A. (2012) 'Histone H2AX phosphorylation: A marker for DNA damage', *Methods in Molecular Biology*, 920: 613–626.

Shi, L., Wen, H. and Shi, X. (2016) 'The histone variant H3.3 in transcriptional regulation and human disease', *Journal of Molecular Biology*. doi: 10.1016/j.jmb.2016.11.019.

Shimada, M., Haruta, M., Niida, H., Sawamoto, K. and Nakanishi, M. (2010) 'Protein phosphatase 1?? 3 is responsible for dephosphorylation of histone H3 at Thr 11 after DNA damage', *EMBO Reports*, 11(11): 883–889.

Sievers, F. and Higgins, D. G. (2014) 'Clustal Omega, Accurate Alignment of Very Large Numbers of Sequences', in. Humana Press, Totowa, NJ, pp. 105–116. doi: 10.1007/978-1-62703-646-7_6.

Sinha, A., Hughes, K. R., Modrzynska, K. K., Otto, T. D., Pfander, C., Dickens, N. J., Religa, A. A., Bushell, E., Graham, A. L., Cameron, R., Kafsack, B. F. C., Williams, A. E., Llinas, M., Berriman, M., Billker, O. and Waters, A. P. (2014) 'A cascade of DNA-binding proteins for sexual commitment and development in *Plasmodium*', *Nature*, 507(7491): 253–257.

Stilger, K. L. and Sullivan, W. J. (2013) 'Elongator protein 3 (Elp3) lysine acetyltransferase is a tail-anchored mitochondrial protein in *toxoplasma gondii*', *Journal of Biological Chemistry*, 288(35): 25318–25329.

Tonkin, C. J., Carret, C. K., Duraisingh, M. T., Voss, T. S., Ralph, S. A., Hommel, M., Duffy, M. F., Silva, L. M. da, Scherf, A., Ivens, A., Speed, T. P., Beeson, J. G., Cowman, A. F., Da Silva, L. M., Scherf, A., Ivens, A., Speed, T. P., Beeson, J. G. and Cowman, A. F. (2009) 'Sir2 paralogues cooperate to regulate virulence genes and antigenic variation in *Plasmodium falciparum*', *PLoS Biology*, 7(4): 0771–0788.

Trelle, M. B., Salcedo-Amaya, A. M., Cohen, A. M., Stunnenberg, H. G. and Jensen, O. N. (2009) 'Global histone analysis by mass spectrometry reveals a high content of acetylated lysine residues in the malaria parasite *Plasmodium falciparum*', *Journal of Proteome Research*, 8(7): 3439–3450.

Verma, G. and Surolia, N. (2013) '*Plasmodium falciparum* CENH3 is able to functionally complement Cse4p and its, C-terminus is essential for centromere function', *Molecular and Biochemical Parasitology*, 192(1–2): 21–29.

Vermaak, D., Hayden, H. S. and Henikoff, S. (2002) 'Centromere Targeting Element within the Histone Fold Domain of Cid', *Molecular and Cell Biology*, 22(21): 7553–7561.

Volz, J. C. C., Bártfai, R., Petter, M., Langer, C., Josling, G. A. A., Tsuboi, T., Schwach, F., Baum, J., Rayner, J. C. C., Stunnenberg, H. G. G., Duffy, M. F. F. and Cowman, A. F. F. (2012) 'PfSET10, a *Plasmodium falciparum* Methyltransferase, Maintains the Active *var* Gene in a Poised State during Parasite Division', *Cell Host & Microbe*, 11(1): 7–18.

Volz, J., Carvalho, T. G., Ralph, S. A., Gilson, P., Thompson, J., Tonkin, C. J.,

Langer, C., Crabb, B. S. and Cowman, A. F. (2010) 'Potential epigenetic regulatory proteins localise to distinct nuclear sub-compartments in *Plasmodium falciparum*', *International Journal for Parasitology*, 40(1): 109–121.

Wang, A. Y., Aristizabal, M. J., Ryan, C., Krogan, N. J. and Kobor, M. S. (2011) 'Key Functional Regions in the Histone Variant H2A.Z C-Terminal Docking Domain', *Molecular and Cellular Biology*, 31(18): 3871–3884.

Wang, C. Y., Hua, C. Y., Hsu, H. E., Hsu, C. L., Tseng, H. Y., Wright, D. E., Hsu, P. H., Jen, C. H., Lin, C. Y., Wu, M. Y., Tsai, M. D. and Kao, C. F. (2011) 'The C-terminus of histone H2B is involved in chromatin compaction specifically at telomeres, independently of its monoubiquitylation at lysine 123', *PLoS ONE*, 6(7). doi: 10.1371/journal.pone.0022209.

Zhu, A. Y., Zhou, Y., Khan, S., Deitsch, K. W., Hao, Q. and Lin, H. (2012) '*Plasmodium falciparum* Sir2A preferentially hydrolyzes medium and long chain fatty acyl lysine', *ACS Chemical Biology*, 7(1): 155–159.